

## **CHAPTER 9**

# **Analytical Methods for Determining Fire Resistance of Steel Members**

---

*James A. Milke*

---

### **Introduction**

Traditionally, fire resistance has been evaluated by subjecting a structural member to a standard test for a specified duration.<sup>1</sup> All members performing acceptably are rated and listed for the duration period of the test (e.g., 1 hr, 2 hr). Assemblies not listed are assumed to be unable to meet the test criteria and, thus, have no rating, unless proved otherwise. Providing proof of acceptable performance can be accomplished in one of three manners:

1. Conduct the standard test.<sup>1</sup>
2. Conduct a special experiment.<sup>2</sup>
3. Apply an analytical technique.<sup>3</sup>

The standard test can involve an appreciable turnaround time in order to specify, schedule, and analyze the results of the test. An experimental program can require a substantial amount of effort in order to obtain accurate data. The costs involved in sponsoring a standard test or experimental program can be appreciable. In the case of archaic structural assemblies, materials may no longer be available to reconstruct the design for possible testing.

Because of these drawbacks, calculation methods have been developed to analyze structural designs for fire conditions. The calculation methods have been formulated based on analyses of data from standard tests, experimental programs, and theoretically based investigations.

Analytical methods for fire resistance must consider three basic aspects of the problem:

1. Fire exposure
2. Heat transfer
3. Structural response

The fire exposing the structure must be characterized using methods described in other chapters of this hand-

book for the case of a real fire, or by assuming the fire exposure specified in the standard test. The thermal response of the structural member can be addressed using principles of heat transfer. Heating within the member is treated by conduction heat transfer analysis (radiation and convection heat transfer may also need to be considered, if voids or porous insulation materials are present within the assembly). Typically, radiative and convective boundary conditions are present. Finally, the structural response is examined by comparing some or all of the following: deflections, strains, and stress levels to established limits.

The following types of calculation methods are available to assess the fire resistance of steel structural members:

1. Empirical correlations
2. Heat transfer analyses
3. Structural analyses

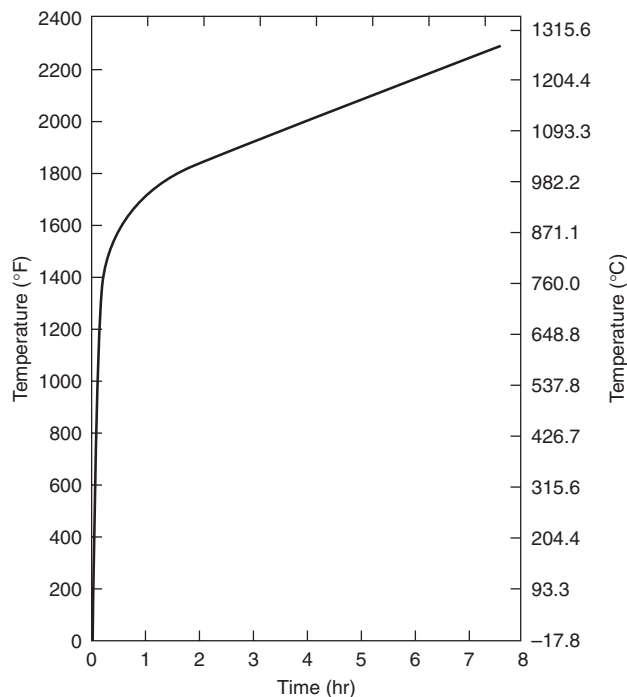
Empirical correlations are based on the analysis of data resulting from performing the standard test numerous times. A limitation of the empirical correlations is that they can only be applied when considering the fire exposure, loading, and span provided in the standard test. If other conditions apply, then another approach is needed.

The second group of calculation methods consists of heat transfer analyses. The heat exposure conditions may be those associated with the standard test or a specified fire. The purpose of the heat transfer analysis is to determine the time required for the structural member to attain a predetermined critical temperature or to provide input to a structural analysis. The temperature endpoint criteria cited by ASTM E119<sup>1</sup> are often accepted as the critical temperatures. Typically, inaccuracies of this method are related to the temperature dependence of the material properties or the description of the heating conditions.

Many of the structural analysis-based calculations are similar to those conducted for structural engineering purposes, except the material properties are evaluated at elevated temperatures and thermal expansion is considered. In structural analyses, the loading and end conditions must be known or assumed. Limitations result from

---

James A. Milke is an associate professor in the Department of Fire Protection Engineering at the University of Maryland. His recent research activities have included the impact of fires on the structural response of steel and advanced composite members.



**Figure 4-9.1. ASTM E119 standard time-temperature curve.<sup>1</sup>**

uncertainties in characterizing the end conditions and the material properties at elevated temperatures.

This chapter provides an overview of the available calculation methods for determining the fire resistance of steel structural members. The basis of each method will be presented along with sample applications.

### Standard Test for Fire Resistance of Structural Members

The standard test method in the United States for determining the fire resistance of columns, floor and roof assemblies, and walls is ASTM E119.<sup>\*1</sup> Basically, the test involves subjecting the structural component to a heated furnace environment for the desired duration. If the endpoint criteria are not reached prior to the end of the test period, the assembly passes the test and is rated.

Gas burners are used to heat the furnace in testing laboratories throughout North America. The furnace is heated so that the temperature inside the furnace follows the time-temperature curve illustrated in Figure 4-9.1. In principle, the time-temperature curve is intended to relate to a severe exposure from a room fire. Thus, the applicability of the test method to examine the fire resistance of exterior structural members exposed to fires outside of the building is questionable.<sup>4</sup>

Assemblies may be tested with or without load. If tested under load, the assembly is subjected to maximum

design stress levels, based on common structural analysis procedures for ambient temperature design. Floor and roof assemblies and bearing walls are always tested under load. Columns are tested with or without a loading. Steel beams and girders may be tested without load if the design loading cannot be achieved in the laboratory.

Structural assemblies may be restrained or unrestrained against thermal expansion. The effect of restraint on the fire resistance of assemblies has been investigated by Bletzacker.<sup>4</sup> The degree of restraint in structural members varies with the geometry, connection method, and framing system, among other factors. The descriptions presented in Table 4-9.1 relate actual construction conditions to the restrained and unrestrained designation noted in the ASTM E119 test method.

The minimum dimensions of the structural components for testing are specified in ASTM E119. A maximum set of dimensions is established by the size of available test furnaces. While the test is large-scale, the test cannot be considered full-scale, given the stipulation of the maximum permissible dimensions. The consequence of not testing full-scale members means that continuous beams, actual floor/roof ASTM assemblies, and long columns are not tested. Consequently, this test is only comparative in nature and cannot be used to assess actual performance.

The ASTM E119 endpoint criteria for building assemblies consider structural integrity, temperature, passage of flame, ignition of cotton waste, and in some cases, response to the hose stream. For the tests without loading, the structural integrity endpoint criterion is relaxed to require that the component only remains in place. The structural integrity criterion addresses the need for members to remain in place (supporting self-weight of member) and to continuously support any applied loads. The ignition-of-cotton-waste endpoint addresses the ability of the structural assembly to prevent the transmission of flame and hot gases to the side not exposed to the furnace fire.

The temperature endpoint criteria are noted in Table 4-9.2. In principle, the endpoint temperatures are based on the maximum allowable reduction in load-bearing capacity of the structural member, based on the reduction in strength experienced at elevated temperature and the maximum permissible loads stipulated by structural design standards.

### Fire Resistance of Steel Members

Several calculation techniques are available to determine the fire resistance of steel members, including steel columns, beams in floor and roof assemblies, and trusses.<sup>7-10</sup> Three types of techniques are available: empirically derived correlations, heat transfer analyses, and structural analyses.

The equations and models do not eliminate the need for all future testing. Testing is still required, at least to validate the calculation techniques and assess the interaction and mechanical behavior of the constituents of the assembly, such as the steel structural member, insulating materials, or other components. However, the calculation techniques can be used to extend the application of test results and reduce the number of required tests. In addi-

<sup>\*Versions of the test method are also published as NFPA 251<sup>5</sup> and UL 263.<sup>6</sup></sup>

**Table 4-9.1 Restrained and Unrestrained Construction Systems (from ASTM E119 Table X3.1)<sup>1</sup>**

<b>Wall bearing:</b>	
Single span and simply supported end spans of multiple bays: <sup>a</sup>	
Open-web steel joists or steel beams, supporting concrete slab, precast units, or metal decking	unrestrained
Concrete slabs, precast units, or metal decking	unrestrained
Interior spans of multiple bays:	
Open-web steel joists, steel beams or metal decking, supporting continuous concrete slab	restrained
Open-web steel joists or steel beams, supporting precast units or metal decking	unrestrained
Cast-in-place concrete slab systems	restrained
Precast concrete where the potential thermal expansion is resisted by adjacent construction <sup>b</sup>	restrained
<b>Steel framing:</b>	
Steel beams welded, riveted or bolted to the framing members	restrained
All types of cast-in-place floor or roof systems (such as beam-and-slabs, flat slabs, pan joists, and waffle slabs) where the floor or roof system is secured to the framing members	restrained
All types of prefabricated floor or roof systems where the structural members are secured to the framing members and the potential thermal expansion of the floor or roof system is resisted by the framing system or the adjoining floor or roof construction <sup>b</sup>	restrained
<b>Concrete framing:</b>	
Beams securely fastened to the framing members	restrained
All types of cast-in-place floor or roof systems (such as beam-and-slabs, flat slabs, pan joists, and waffle slabs) where the floor system is cast with the framing members	restrained
Interior and exterior spans of precast systems with cast-in-place joints resulting in restraint equivalent to that which would exist in condition III(1)	restrained
All types of prefabricated floor or roof systems where the structural members are secured to such systems and the potential thermal expansion of the floor or roof systems is resisted by the framing system or the adjoining floor or roof construction <sup>b</sup>	restrained
<b>Wood construction:</b>	
All types	unrestrained

<sup>a</sup>Floor and roof systems can be considered restrained when they are tied into walls with or without tie beams, the walls being designed and detailed to resist thermal thrust from the floor or roof system.

<sup>b</sup>For example, resistance to potential thermal expansion is considered to be achieved when:

1. Continuous structural concrete topping is used
2. The space between the ends of precast units or between the ends of units and the vertical face of supports is filled with concrete or mortar, or
3. The space between the ends of precast units, and the vertical faces of supports, or between the ends of solid or hollow core slab units, does not exceed 0.25% of the length for normal-weight concrete members or 0.1% of the length for structural lightweight concrete members.

**Table 4-9.2 ASTM E119 Temperature Endpoint Criteria<sup>1</sup>**

Structural Member	Location	Maximum Temperature °C (°F)*
Walls/partitions (bearing and nonbearing)	1. Unexposed side	
	Average	139 (250) <sup>a</sup>
	Single point	181 (325) <sup>a</sup>
Steel columns	1. Average	538 (1000)
	Single point	649 (1200)
Floor/Roof assemblies and loaded beams	1. Average	538 (1000)
	Single point	649 (1200)
	1. Unexposed side	
	Average	139 (250) <sup>a</sup>
	Single point	181 (325) <sup>a</sup>
	2. Steel beam	
	Average	593 (1100)
	Single point	704 (1300)
	3. Pre-stressing steel	426 (800)
	4. Reinforcing steel	593 (1100)
	5. Open-web steel joists	593 (1100)
Steel beams/girders (not loaded)	1. Average	538 (1000)
	Single point	649 (1200)

\*Maximum temperature cited refers to the maximum temperature rise above initial conditions

tion, experimental methods are essential in determining the material properties at elevated temperature of the protection materials.

### Steel Material Properties

The principal material properties of interest are yield strength, ultimate strength, modulus of elasticity, coefficient of thermal expansion, density, specific heat, and thermal conductivity. The effect of temperature on steel properties has been examined by many researchers.<sup>11</sup> For steel, all of the properties, except for density, are strongly influenced by temperature.

The thermal properties of ASTM A36 steel are provided in the following correlations:<sup>7,12,13,14</sup>

$$k = -0.022T + 48 \quad \text{for } 0 \leq T \leq 900^\circ\text{C}$$

$$k = 28.2 \quad \text{for } 900^\circ\text{C} < T$$

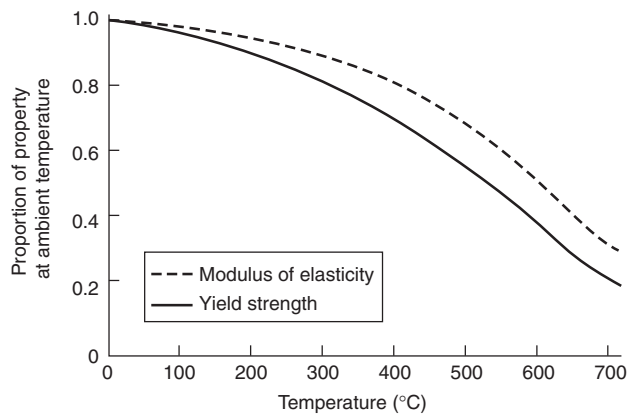
$$c_s = 0.51T + 420 \quad \text{for } 0 \leq T \leq 650^\circ\text{C}$$

$$c_s = 8.65T + 4870 \quad \text{for } 650^\circ\text{C} < T \leq 725^\circ\text{C}$$

$$c_s = -10.9T + 9340 \quad \text{for } 725^\circ\text{C} < T \leq 800^\circ\text{C}$$

$$c_s = 579 \quad \text{for } 800^\circ\text{C} < T$$

$$\rho = 7860 \text{ kg/m}^3$$



**Figure 4-9.2. Temperature effects on properties of ASTM A36 steel.**<sup>12,15</sup>

The influence of temperature on the mechanical properties of A36 steel is presented in Figure 4-9.2. At 538°C (1000°F), the yield strength is approximately 60 percent of the value at normal room temperature. The American Institute for Steel Construction's *Specification for the Design, Fabrication, and Erection of Structural Steel for Buildings*<sup>16</sup> limits the maximum permissible design stress to approximately 60 percent of the yield strength. Thus, for structural members at 538°C (1000°F) designed to carry the maximum permissible stress, the applied stress is approximately the same as the strength of the member. It should also be noted that at 538°C (1000°F) the modulus of elasticity has decreased appreciably from the value at normal room temperature.

Mathematical expressions describing the relationship of the yield strength, modulus of elasticity, and coefficient of thermal expansion on temperature are<sup>7,17,18</sup>

For  $0 < T \leq 600^\circ\text{C}$ ,

$$\sigma_{yT} = \left[ 1 + \frac{T}{900 \ln(T/1750)} \right] \sigma_{y0}$$

$$E_T = \left[ 1 + \frac{T}{2000 \ln(T/1100)} \right] E_0$$

For  $T > 600^\circ\text{C}$ ,

$$\sigma_{yT} = \frac{340 - 0.34T}{T - 240} \sigma_{y0}$$

$$E_T = \frac{690 - 0.69T}{T - 53.5} E_0$$

$$\alpha_T = (0.004T + 12) \times 10^{-6}$$

where

$\sigma_{yT}$  = yield strength at temperature  $T$  (MPa) (psi)

$\sigma_{y0}$  = yield strength at 20°C (68°F) (MPa) (psi)

$E_T$  = modulus of elasticity at temperature  $T$  (MPa) (psi)

$E_0$  = modulus of elasticity at 20°C (68°F) (MPa) (psi)

$\alpha_T$  = coefficient of thermal expansion at temperature  $T$  (m/m°C)

$T$  = steel temperature (°C)

$$\theta = \frac{T' - 68}{1800} \quad T' \text{ in } ^\circ\text{F}$$

$$\theta = \frac{T' - 20}{1000} \quad T' \text{ in } ^\circ\text{C}$$

$T'$  = steel temperature

In addition to the changes in material properties that occur at elevated temperatures, the crystalline structure of steel also changes, as noted in Figure 4-9.3.<sup>19</sup> However, for the low-carbon steels typically used in building construction, significant changes in crystalline structure only begin to occur at temperatures in excess of 650°C (1200°F),<sup>20</sup> above the temperature typically associated with failure.

Creep, the time-dependent deformation of a material, may be significant in structural steel at temperatures in excess of 460°C (860°F).<sup>21</sup> The rate of creep increases approximately 300 times for ASTM A36 structural steel, when the steel temperature is increased from 460 to 520°C (860 to 968°F). Since creep is a complex phenomenon depending on the stress level, rate of heating, and other factors, often it is included implicitly in the mechanical properties to simplify the fire resistance calculations.<sup>15,20</sup> In-depth discussions of creep have been prepared by Harmathy.<sup>22,23</sup>

## Methods of Protection

The basic intent of the various methods of protection is to reduce the rate of heat transfer to the structural steel. This is accomplished by using insulation, membranes, flame shielding, and heat sinks.

### Insulation

Insulation of the steel is achieved by surrounding the steel with materials that preferably have the following characteristics:<sup>24</sup>

1. Noncombustibility and the added attribute of not producing smoke or toxic gases when subjected to elevated temperatures
2. Thermal protective capability when tested in accordance with the standard fire test ASTM E119
3. Product reliability giving positive assurance of consistent uniform protection characteristics
4. Availability in a form that permits efficient and uniform application
5. Sufficient bond strength and durability to prevent either dislodgement or surface damage during normal construction operations
6. Resistance to weathering or erosion resulting from atmospheric conditions

In addition to the insulating qualities of the protection materials, chemical reactions may occur in the insulation, further reducing the rate of heat transfer. The chemical reactions include calcination, ablation, intumescence, thermal hydrogenation, and sublimation.

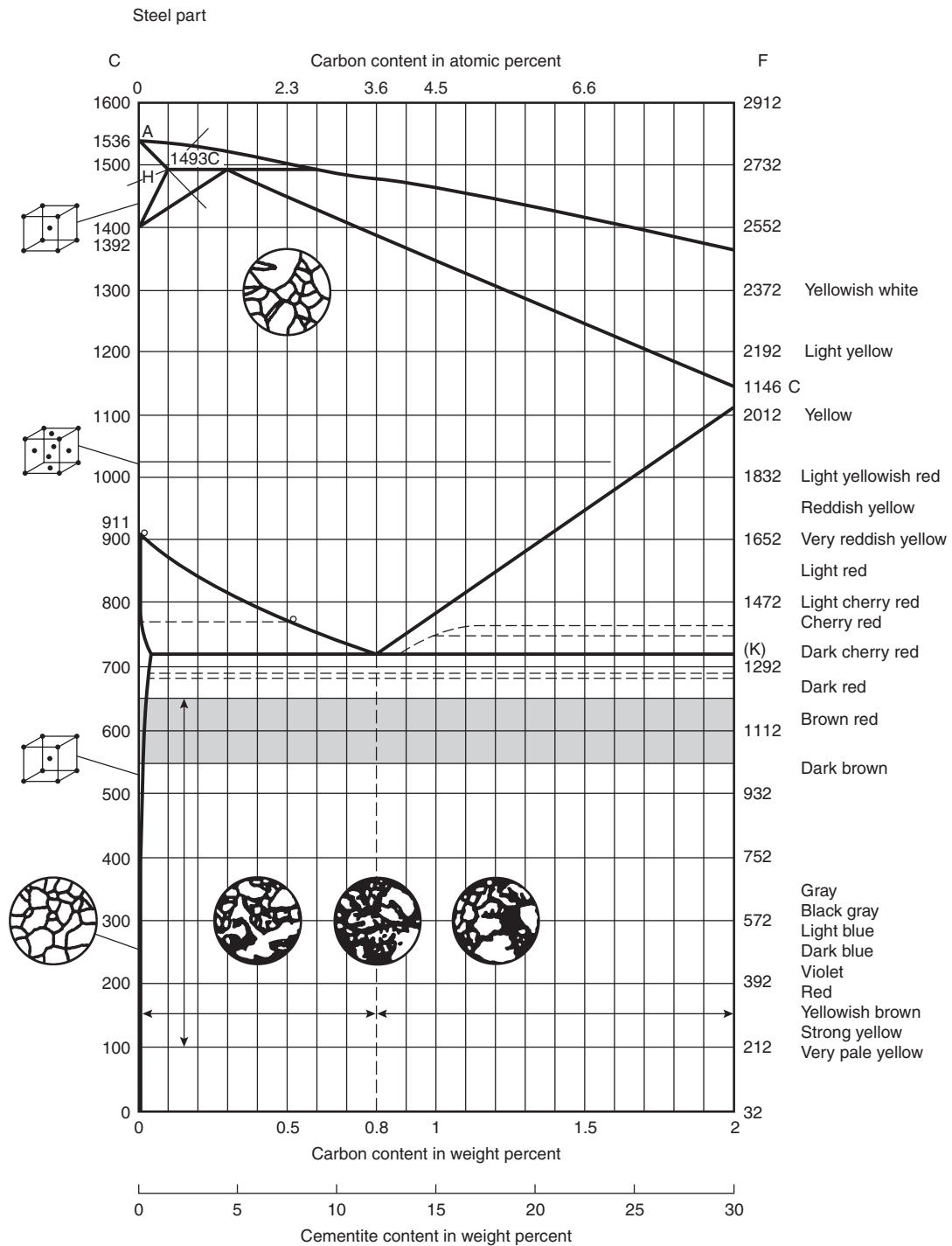


Figure 4-9.3. Influence of elevated temperatures versus carbon content in steel.<sup>19</sup>

Insulating methods include the use of board products, spray-applied materials, and concrete encasement. A brief review of each method is presented below.

**Board products:** Four types of board products are commonly used to protect structural steel: gypsum board, fiber-

reinforced calcium silicate board, vermiculite-sodium silicate board, and mineral fiber board. In each case, the means of attachment of the boards surrounding the steel is a critical parameter affecting the performance of the assembly. Two commonly used methods of attachment of gypsum wallboard with and without steel covers are illustrated in

Figure 4-9.4. Detailed descriptions of the attachment mechanisms for the other board products are provided elsewhere.<sup>25-27</sup> Also, board products can be used in wall assemblies to provide an envelope around steel trusses.

**Spray-applied materials:** Several types of spray-applied materials are commonly used. These include cementitious plasters, mineral fibers, magnesium oxychloride cements, and intumescent. Sufficient data has been obtained to characterize spray-applied cementitious and mineral fiber materials for the purpose of estimating the fire endurance of structural steel protected with these materials. An illus-

tration of a steel column protected by a spray-applied material is presented in Figure 4-9.5.

**Concrete encasement:** Concrete encasement of steel members to surround and insulate the steel is illustrated in Figure 4-9.6. As indicated in Figure 4-9.6, the concrete is cast to fill in all re-entrant spaces. Alternatively, concrete column covers may be used, as illustrated in Figure 4-9.7. The concrete is assumed to act only to thermally protect the steel. Some empirical correlations implicitly account for the load-bearing capacity of the concrete and possible steel-concrete composite action.

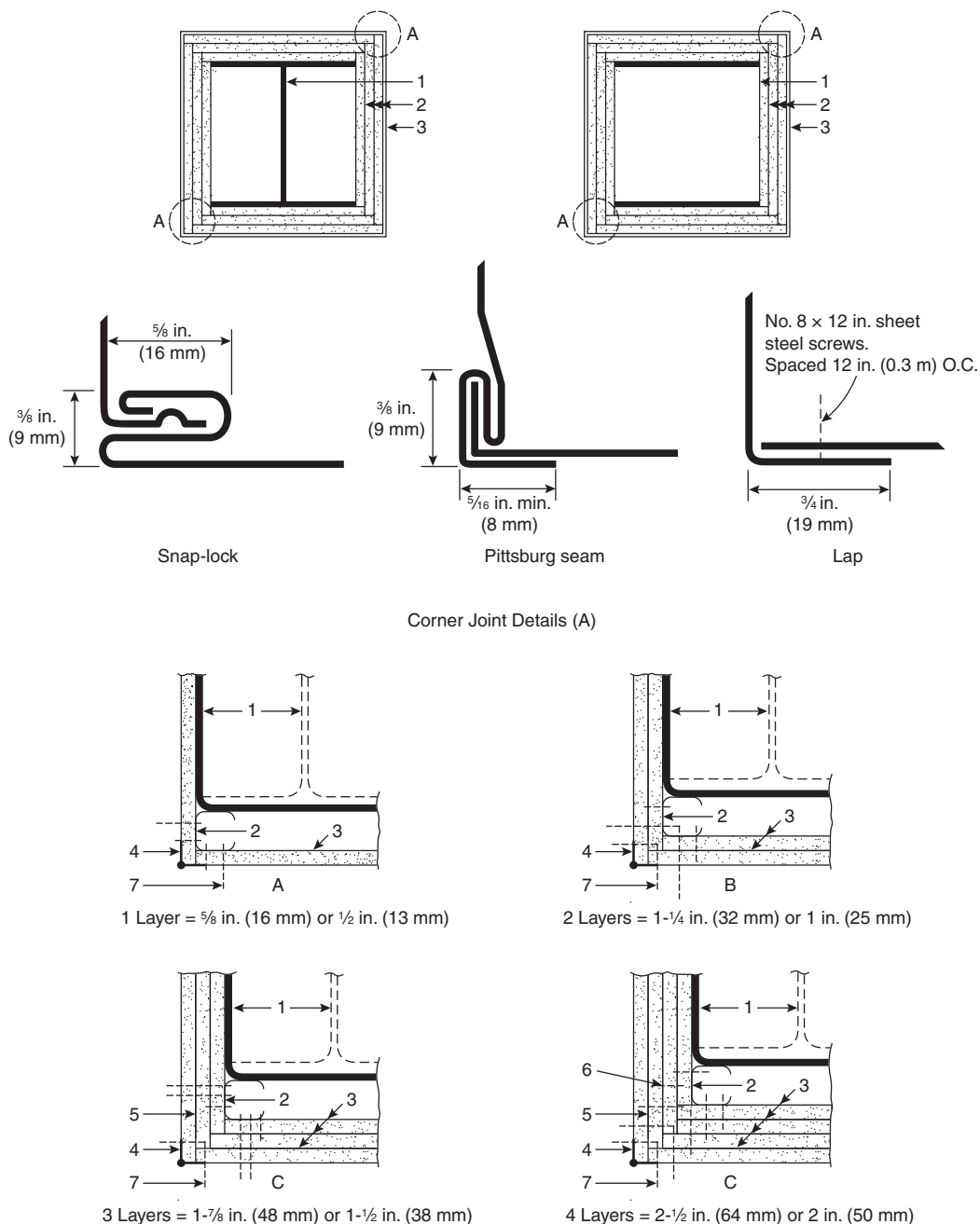


Figure 4-9.4. Attachment mechanisms of gypsum wallboard to steel columns.<sup>25</sup>



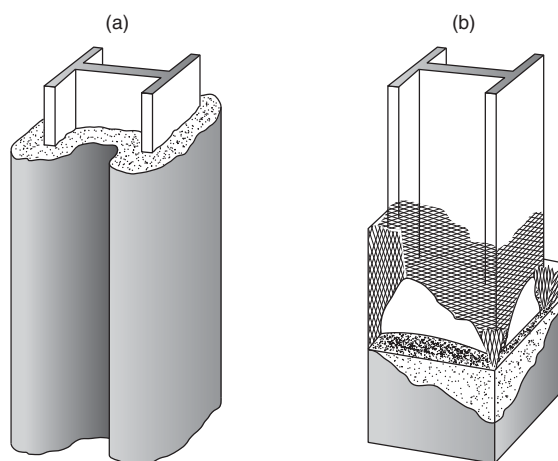


Figure 4-9.5. (a) Sprayed insulation; (b) Metal lath and plaster encasement.<sup>24</sup>

**Membrane:** Suspended ceiling assemblies are used as membranes to protect structural steel in floor and roof assemblies. The ceiling panels and tiles comprising the ceiling assembly may consist of gypsum, perlite, vermiculite, or mineral fibers.

The membrane method of protection is illustrated in Figure 4-9.8. Heat transfer to the structural steel is reduced due to the air space above the membrane and the insulating characteristics of the membrane. Also, membranes help prevent the direct impingement of flame on the structural steel.

**Flame shield:** Flame shields are intended to reduce the incident radiant heat flux on the steel by preventing direct flame impingement. The effectiveness of flame shields to protect exposed spandrel beams was first examined by Seigel.<sup>2,28</sup> In this instance, 14-gage sheet steel was used as the flame shield.

**Heat sinks:** The heat sink approach delays the heating of steel by absorbing heat transferred through the steel. The heat sink approach usually involves liquid- or concrete-

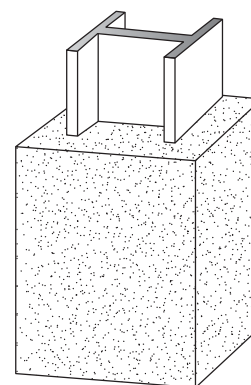


Figure 4-9.6. Steel column with concrete encasement.<sup>24</sup>

filling of the interior of hollow steel members (tubular and pipe sections). Liquid-filling can be used to provide a sufficient level of protection for the columns, without any externally applied coating. The liquid used for protection is an aqueous solution. Additives are provided primarily for antifreeze, corrosion protection, and biological reasons.

A diagram of a typical design for a liquid-filled column fire protection system is presented in Figure 4-9.9. The components of this system include the hollow structural steel columns, piping to connect the columns, a water storage tank, and associated valves.

The system operates on the principle that heat incident on the column is removed by circulation of the liquid. If sufficient heat is delivered to the liquid, boiling can be expected, which enhances the efficiency of the heat-removal process. In many tests with liquid-filling, steel temperatures have been observed to be well below those required for failure, as long as the column remains full of the liquid.

Another heat-sink approach consists of filling the interior of hollow steel columns with concrete. If the concrete is reinforced, load transfer from the steel to the concrete can be expected as the steel weakens with increasing temperature. Calculation methods to determine the fire resistance of concrete-filled steel columns are available.<sup>10,12</sup>

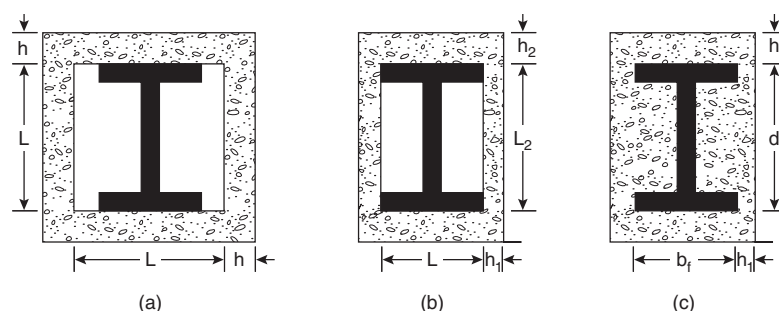
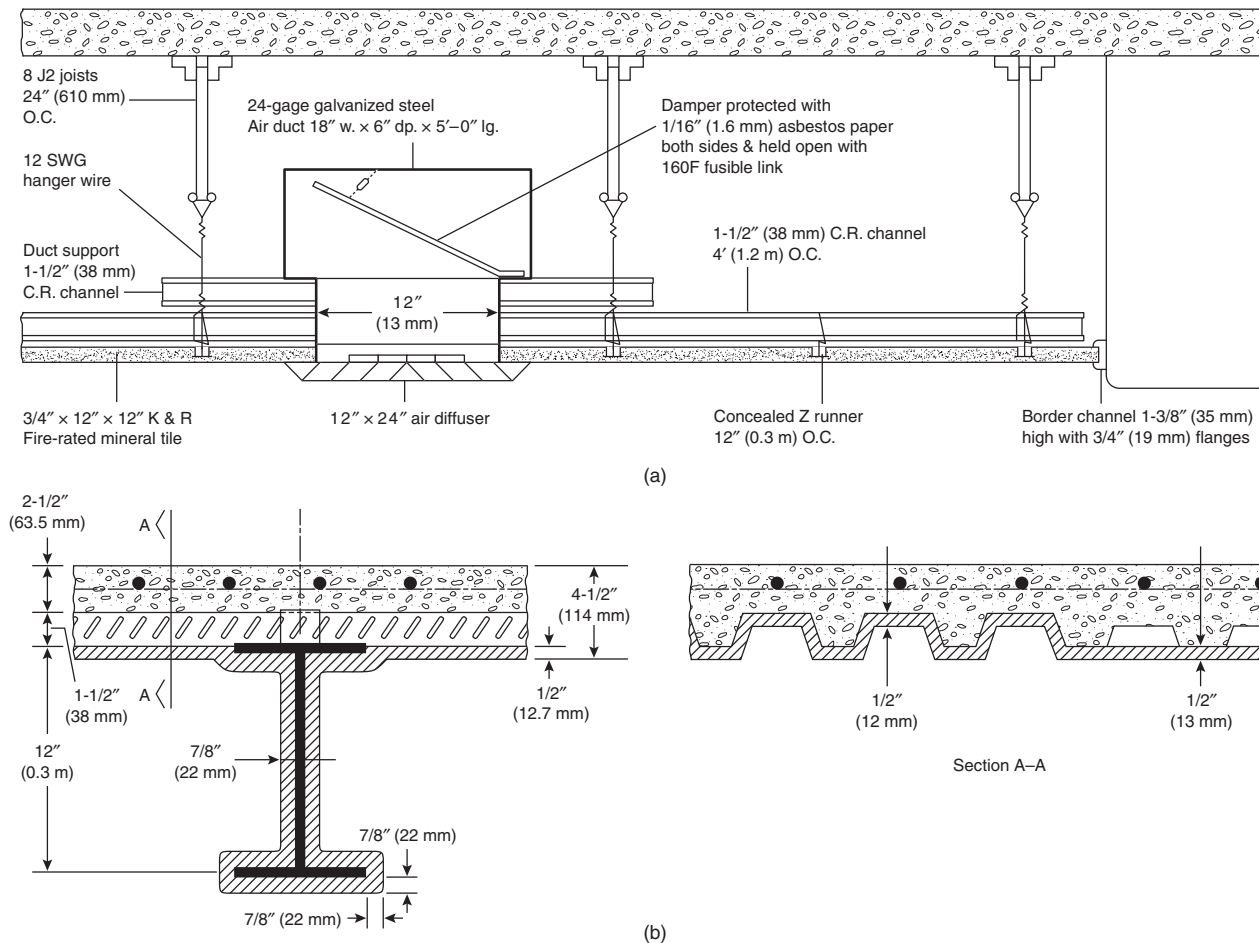


Figure 4-9.7. Concrete-protected structural steel columns. (a) Square shape protection with a uniform thickness of concrete cover on all sides; (b) Rectangular shape with varying thickness of concrete cover; and (c) Encasement having all re-entrant spaces filled with concrete.



**Figure 4-9.8. Membrane method of protection,<sup>24</sup> (a) Cross-section of a floor-ceiling system with conventional sheet steel fusible-link damper for protecting typical ceiling outlets in galvanized sheet ducts; (b) Sprayed contact fireproofing applied directly to the underside of formed-steel decking and to a supporting steel beam.**

## Empirically Derived Correlations

Numerous, easy-to-use, empirically derived correlations are available to calculate the fire resistance of steel columns, beams, and trusses. The correlations are based on data from performing the standard test numerous times on variations of a particular assembly. Curve-fitting techniques are used to establish the various correlations. In some cases, a best-fit line has been drawn for the data points, whereas in other cases, lines were placed to provide conservative estimates of the fire endurance by connecting the two lowest points.<sup>29</sup>

## Steel Columns

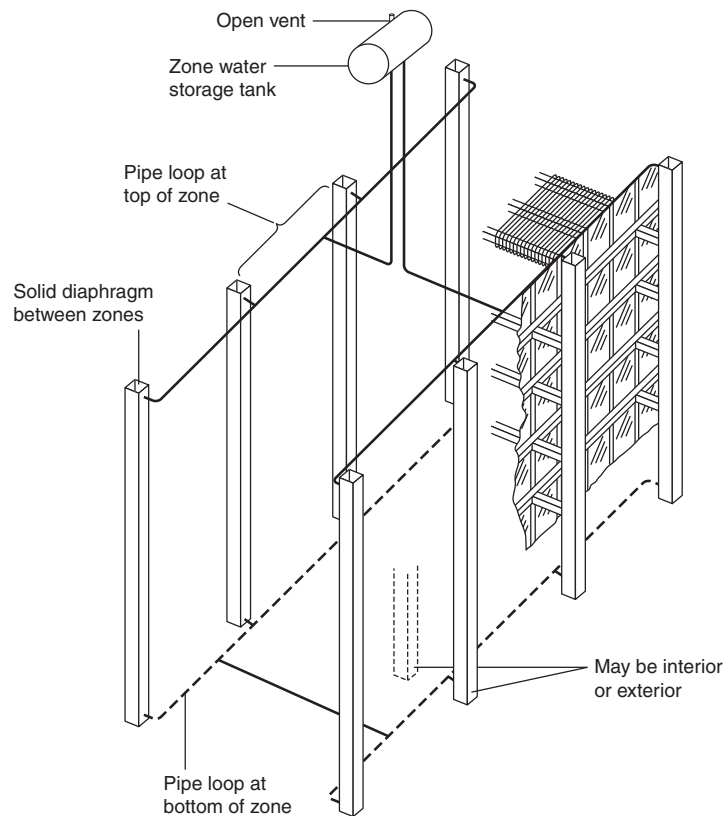
The correlations to estimate the fire endurance of unprotected and protected steel columns are given in Table 4-9.3. Present in each of the equations is  $W/D$  for wide-flange sections and  $A/P$  for hollow sections. The  $W/D$

and  $A/P$  ratios are comparable. The  $W/D$  ratio is the weight per lineal foot to the heated perimeter of the steel at the protection interface (or the perimeter of the steel if unprotected). The  $A/P$  ratio is the cross-sectional area divided by the heated perimeter. Essentially, the  $W/D$  ratio relates to the product of the density of the steel and the  $A/P$  ratio.

The relevance of the  $W/D$  and  $A/P$  ratios was first noted by Lie and Stanzak.<sup>30</sup>  $W/D$  ratios for commonly used wide-flange and tubular shapes for columns and beams are available elsewhere.<sup>25,31,32</sup> The two factors in the  $W/D$  ratio that affect the rate of heat transfer to the steel (and consequently the rise in temperature of the steel) are (1) shape of the fire protection system,  $D$ , and (2) steel mass per unit of length,  $W$ .

The parameter that characterizes the shape of the fire protection system is  $D$ , the heated perimeter expressed in inches, which is defined as the inside perimeter of the steel at the fire protection material interface. Figure 4-9.10 illustrates the method for determining  $D$  in four typical





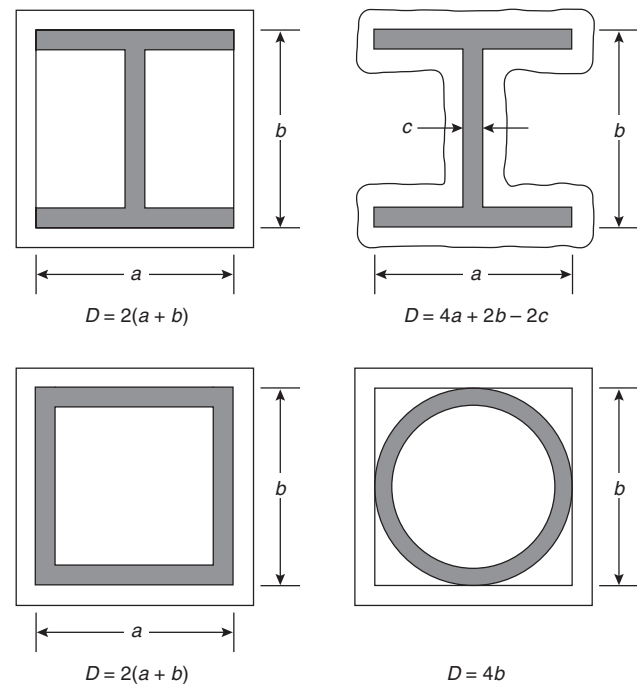
**Figure 4-9.9. Schematic layout of a typical piping arrangement used in a liquid-filled column fire-protection system.<sup>4</sup>**

cases. As can be seen from the figure, the heated perimeter depends on the size of the column and also on the profile of the protection system. Two different commonly used profiles are: (1) contour profile, where all surfaces of the steel column are in contact with the protection material and (2) box profile, where a rectangular box of protection material is built around the column.

A large value of  $W$  refers to a column with a large weight per lineal foot. A given amount of energy will raise the temperature of the massive column to a lesser degree than that of a light column. Less surface area is available for heat transfer if the heated perimeter,  $D$ , is small, thereby inhibiting the temperature rise in the steel. The greater the  $W/D$  ratio, the greater the inherent fire resistance of the assembly is.

Because steel elements with larger  $W/D$  ratios are inherently more fire resistant, substituting shapes with greater  $W/D$  ratios for shapes identified in the listed designs in the *UL Fire Resistance Directory*<sup>3</sup> is permitted while maintaining the same thickness of protection. However, such substitution yields inefficient designs, because shapes with large  $W/D$  ratios actually require less fire protection material than shapes with small  $W/D$  ratios for the same level of fire resistance.

The equation for gypsum wallboard protection is nonlinear. The weight of the gypsum wallboard is included because the heat capacity of gypsum has a considerable



**Figure 4-9.10. Heated perimeter for steel columns.<sup>25</sup>**

**Table 4-9.3 Empirical Equations for Steel Columns<sup>20,26,27</sup>**

Member/Protection	Solution	Symbols
Column/Unprotected	$R = 10.3 (W/D)^{0.7}$ , for $W/D < 10$ $R = 8.3 (W/D)^{0.8}$ , for $W/D \geq 10$ (for critical temperature of 1000°F)	$R$ = fire endurance time (min) $W$ = weight of steel section per linear foot (lb/ft) $D$ = heated perimeter (in.)
Column/Gypsum Wallboard	$R = 130 \left( \frac{hW'/D}{2} \right)^{0.75}$ where $W' = W + \left( \frac{50hD}{144} \right)$	$h$ = thickness of protection (in.) $W'$ = weight of steel section and gypsum wallboard (lb/ft)
Column/Spray-applied materials and board products—wide flange shapes	$R = [C_1(W/D) + C_2]h$	$C_1$ & $C_2$ = constants for specific protection material
Column/Spray-applied materials and board products—hollow sections	$R = C_1 \left( \frac{A}{P} \right) h + C_2$	$C_1$ & $C_2$ = constants for specific protection material The $A/P$ ratio of a circular pipe is determined by $A/P \text{ pipe} = \frac{t(d-t)}{d}$ where $d$ = outer diameter of the pipe (in.) $t$ = wall thickness of the pipe (in.) The $A/P$ ratio of a rectangular or square tube is determined by $A/P \text{ tube} = \frac{t(a+b-2t)}{a+b}$ where $a$ = outer width of the tube (in.) $b$ = outer length of the tube (in.) $t$ = wall thickness of the tube (in.)
Column/Concrete cover	$R = R_0(1 + 0.03m)$ where $R_0 = 10(W/D)^{0.7} + 17 \left( \frac{h^{1.6}}{k_c^{0.2}} \right) \cdot \left\{ 1 + 26 \left[ \frac{H}{\rho_c c_c h(L+h)} \right]^{0.8} \right\}$ $D = 2(b_f + d)$	$R_0$ = fire endurance at zero moisture content of concrete (min.) $m$ = equilibrium moisture content of concrete (% by volume) $b_f$ = width of flange (in.) $d$ = depth of section (in.) $k_c$ = thermal conductivity of concrete at ambient temperature (Btu/hr·ft·°F) $h$ = thickness of concrete cover (in.)
Column/Concrete encased	for concrete-encased columns use $H = 0.11W + \frac{\rho_c c_c}{144}(b_f d - A_s)$ $D = 2(b_f + d)$ $L = (b_f + d)/2$	$H$ = thermal capacity of steel section at ambient temperature (= $0.11W$ Btu/ft·°F) $c_c$ = specific heat of concrete at ambient temperature (Btu/lb·°F) $L$ = inside dimension of one side of <i>square</i> concrete box protection (in.) $A_s$ = cross-sectional area of steel column (in. <sup>2</sup> )

impact on the fire resistance of the assembly. The thickness of wallboard required to achieve a particular level of fire resistance as a function of the  $W/D$  ratio of the column is presented in Figure 4-9.10.

Based on an elementary heat transfer analysis, Stanzak and Lie conducted a parametric analysis that resulted in correlations of the following form to estimate the thickness of material required to achieve a particular level of fire resistance:<sup>25,27</sup>

$$R = (C_1 W/D + C_2)h$$

where

$R$  = fire endurance (hr)

$W$  = steel weight per lineal foot (lb/ft)

$D$  = heated perimeter of the steel at the insulation interface (in.)

$h$  = thickness of insulation (in.)

The constants  $C_1$  and  $C_2$  need to be determined for each protection material. The constants take into account the thermal conductivity and heat capacity of the insulation material. Constants for some materials are included in listings in the *UL Fire Resistance Directory*.<sup>3</sup>

Considering the equation for the concrete cover column protection method (see Table 4-9.3),  $R_0$  is the fire endurance of the assembly if the concrete has no moisture content. However, because the fire resistance of concrete-cover over steel columns is known to increase by approximately 3 percent for each 1 percent of moisture,  $R_0$  is multiplied by the  $(1 + 0.03m)$  factor where  $m$  is the equilibrium moisture content of concrete. The parameters  $h$  and  $L$  noted in the equation are shown in Figure 4-9.7. If the protection thickness or column dimensions are not the same in the vertical and horizontal directions, average values are used for  $h$  and  $L$ .

The heat capacity of the concrete must be accounted for in the determination of  $H$  if all re-entrant spaces are filled. (See Figure 4-9.7.) If specific data on the concrete's thermal properties are not available, values given in Table 4-9.4 may be used. Typical densities for normal-weight and lightweight concrete are 145 and 110 lb/ft<sup>3</sup> (2320 and 1760 kg/m<sup>3</sup>). Also, the typical equilibrium moisture content (by volume) for normal-weight concrete is 4 percent and lightweight concrete is 5 percent.

Many of the equations cited in Table 4-9.3 are limited to a range of shapes or protection thickness. Before applying any equation from this table, users should consult the original reference and confirm that the equation is being applied properly.

#### EXAMPLE 1:

Determine the thickness of spray-applied cementitious material to obtain a 2-hr fire endurance when applied to a  $W 12 \times 106$  column.

#### SOLUTION:

From UL X772, the applicable equation is

$$R = (63W/D + 36)h$$

Solving for  $h$ ,

$$h = \frac{R}{63W/D + 36}$$

where

$$R = 2 \text{ hrs} = 120 \text{ min}$$

$W/D = 1.44 \text{ lb/ft-in.}$  for a  $W 12 \times 106$  with contour profile protection

**Table 4-9.4 Thermal Properties of Concrete at 70°F**

	Normal-Weight Concrete	Structural Lightweight Concrete
Thermal conductivity ( $k$ ) <sup>a</sup>	0.95	0.35
Specific heat ( $c$ ) <sup>b</sup>	0.20	0.20

<sup>a</sup>Expressed as Btu/hr·ft·°F

<sup>b</sup>Expressed as Btu/lb·°F

Substituting,

$$h = \frac{120}{63 \times 1.44 + 36} = 0.95 \text{ in.}$$

#### EXAMPLE 2:

Determine the fire endurance of a  $W 8 \times 28$  column encased in lightweight concrete (density of 110 lb/ft<sup>3</sup> [176.2 kg/m<sup>3</sup>]) with all re-entrant spaces filled. The concrete cover thickness is 1.25 in. (31.8 mm).

#### SOLUTION:

From Table 4-9.3, the appropriate equation is

$$R = R_0(1 + 0.03m)$$

where

$$R_0 = 10(W/D)^{0.7} + 17(h^{1.6}/k_c^{0.2})\{1 + 26[H/\rho_c c_c h(L + h)]^{0.8}\}$$

Referring to Figure 4-9.7,

$$h_2 = h_1 = h = 1.25 \text{ in. (31.8 mm)}$$

$$b_f = 6.535 \text{ in. (166 mm)}$$

$$d = 8.060 \text{ in. (204.7 mm)}$$

$$W/D = 0.67 \text{ lb/ft-in. (39.3 kg/m}^2\text{)(contour profile)}$$

$$A = 8.25 \text{ in.}^2 \text{ (0.0053 m}^2\text{)}$$

From Table 4-9.4,

$$k_c = 0.35 \text{ Btu/hr·ft·°F}$$

$$c_c = 0.20 \text{ Btu/lb·°F}$$

$$\rho_c = 110 \text{ lb/ft}^3$$

$$L = \frac{1}{2}(b_f + d) = 7.30 \text{ in.}$$

$$H = 0.11W + \frac{\rho_c c_c}{144}(b_f D - A_s)$$

$$H = 0.11 \times 28 + \frac{110 \times 0.20}{144}(6.535 \times 8.060 - 8.25) = 9.87$$

$$R_0 = 10(0.67)^{0.7} + 17\left(\frac{1.25^{1.6}}{0.35^{0.2}}\right)$$

$$\times \left\{1 + 26\left[\frac{9.87}{110 \times 0.2 \times 1.25(7.30 + 1.25)}\right]^{0.8}\right\}$$

$$R_0 = 99 \text{ min}$$

Assuming a moisture content of 5 percent for lightweight concrete,

$$R = 99(1 + 0.03 \times 5) = 114 \text{ min}$$

#### Steel Beams

As in the case of columns, the  $W/D$  ratio is an important parameter affecting the fire resistance of a beam. Beams with larger  $W/D$  ratios may be substituted for

beams with lesser  $W/D$  ratios for an equivalent rating with no change in the protection thickness. However, as with columns, designs resulting from the direct substitution of larger beams without reducing the protection thickness may be inefficient.

In 1984, an empirically derived correlation was developed to calculate the required thickness of spray-applied material protection.<sup>31</sup> Correlations of the form for steel columns are not possible, given the deck's role as a heat sink. Thus, the thickness of protection for steel beams is determined based on the following scaling relationship:

$$h_1 = \left( \frac{W_2/D_2 + 0.6}{W_1/D_1 + 0.6} \right) h_2 \quad (1)$$

where

$h$  = thickness of spray-applied fire protection (in.)

$W$  = weight of steel beam (lb/ft)

$D$  = heated perimeter of the steel beam (in.) (See Figure 4-9.11)

and where the subscripts

1 = substitute beam and required protection thickness

2 = the beam and protection thickness specified in the referenced tested design or tested assembly

Limitations of this equation are noted as follows:

1.  $W/D \geq 0.37$
2.  $h \geq 3/8$  in. (9.5 mm)
3. The unrestrained beam rating in the referenced tested design or tested assembly is at least 1 hr

It should be noted that the above equation only pertains to the determination of the protection thickness for a beam in a floor or roof assembly. All other features of the assembly, including the protection thickness for the deck, must remain unaltered.

#### EXAMPLE 3:

Calculate the thickness of spray-applied fire protection required to provide a 2-hr fire endurance for a W 12

$\times 16$  beam to be substituted for a W 8  $\times 17$  beam requiring 1.44 in. (36.6 mm) of protection for the same rating.

#### SOLUTION:

The beam substitution correlation, presented as Equation 1, is used.

$$h_1 = \left( \frac{W_2/D_2 + 0.6}{W_1/D_1 + 0.6} \right) h_2$$

where

$$W_2/D_2 = 0.54 \quad \text{for W 8} \times 17$$

$$W_1/D_1 = 0.45 \quad \text{for W 12} \times 16$$

$$h_2 = 1.44$$

$$h_1 = \left( \frac{0.54 + 0.6}{0.45 + 0.6} \right) \times 1.44 = 1.6 \text{ in.}$$

#### Steel Trusses

There are three types of trusses used in buildings: transfer, staggered, and interstitial trusses. Because of the inherent features of each type of truss, some fire protection systems are more appropriate than others.<sup>33</sup>

A load-transfer truss (see Figure 4-9.12) supports loads from more than one floor. The loads may be suspended

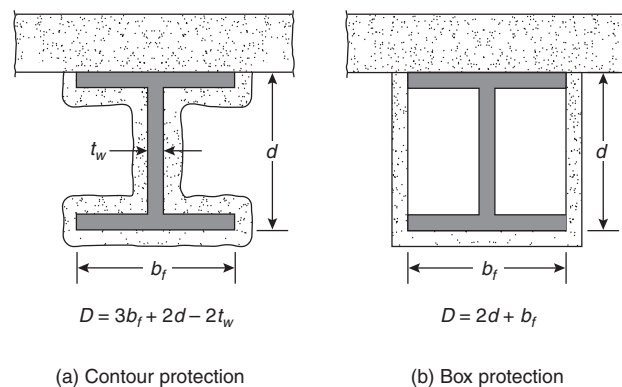


Figure 4-9.11. Heated perimeter for steel beams.<sup>31</sup>

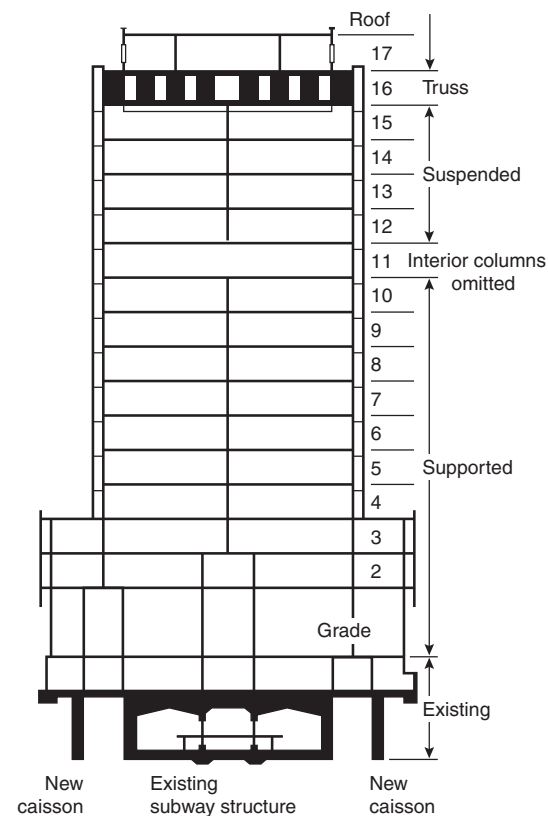


Figure 4-9.12. Vierendell truss providing support from above and below.<sup>33</sup>

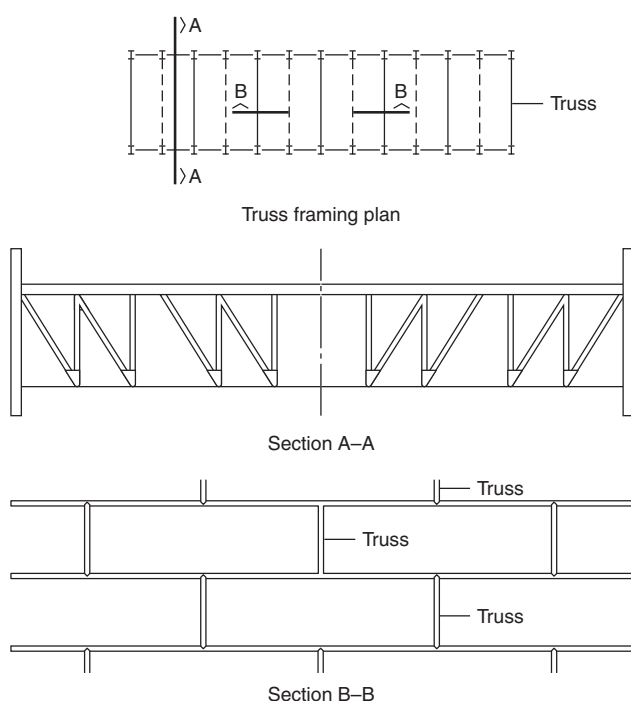
from a transfer truss or the transfer truss can be used to eliminate columns on lower floors.

A staggered truss is illustrated in Figure 4-9.13. Generally, staggered trusses are used in residential occupancy buildings. Staggered trusses carry loads from two floors.

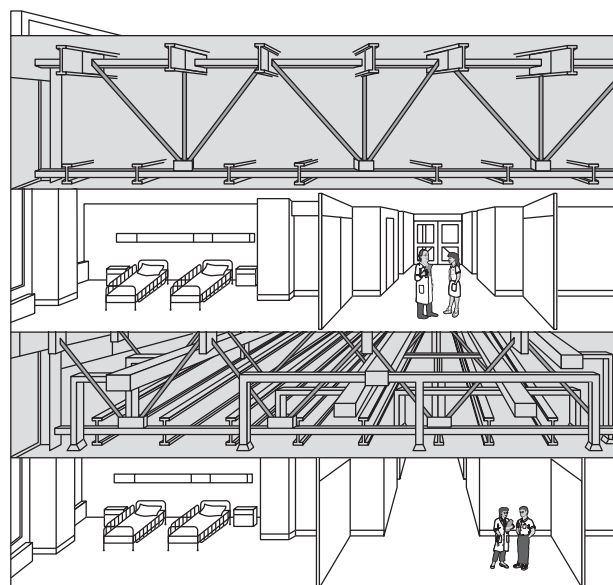
Interstitial trusses are used to create deep floor/ceiling concealed spaces containing mechanical and electrical equipment, as shown in Figure 4-9.14. Interstitial trusses support only those loads from the equipment enclosure and the floor above. Interstitial trusses are typically used in health-care facilities with heavy mechanical equipment needs.

Three methods of fire protection are often used for trusses: membrane, envelope, and individual element protection. Some fire protection methods are more appropriate than others for the specific truss types. The fire protection methods typically used for each truss type are indicated in Table 4-9.5. Membrane protection is accomplished through the use of a fire-resistant ceiling assembly. Design parameters for such an assembly can be determined from listings of fire-rated designs.<sup>3,34</sup> No empirical correlations are available to assess the design of membrane protection systems.

The envelope means of protection is illustrated in Figure 4-9.15. The truss is enclosed in layers of a board product, with the number of layers determined by the required fire endurance. Some practical rules of thumb based on test results are noted in Table 4-9.6.



**Figure 4-9.13. A typical truss and positionings in a staggered truss system.<sup>33</sup>**



**Figure 4-9.14. Hospital interstitial truss system.<sup>33</sup>**

**Table 4-9.5 Typical Fire Protection Methods for Steel Trusses**

Truss Type	Fire Protection Method		
	Membrane	Envelope	Individual Element
Transfer		X	X
Staggered		X	X
Interstitial	X	X	X

**Table 4-9.6 Practical Guidelines for Thickness of Gypsum Wallboard for Steel Truss Envelope Protection<sup>33</sup>**

Fire Endurance	Gypsum X	Wallboard Type
60	5/8" (16 mm)	5/8" (16 mm)
120	1 1/4" (32 mm)	—
180	—	1 1/2" (38 mm)

Individual element protection is generally accomplished using a spray-applied material. Since critical truss elements perform structurally as columns, that is, in tension or compression (as opposed to bending), the applicable equations for determining the thickness of spray-applied material for columns is used. In order to use these equations, the  $W/D$  ratio must be calculated for each element. Unlike columns and beams, the ratio may not be readily available. The diagrams in Figure 4-9.16 are provided for assistance in calculating the heated perimeter.



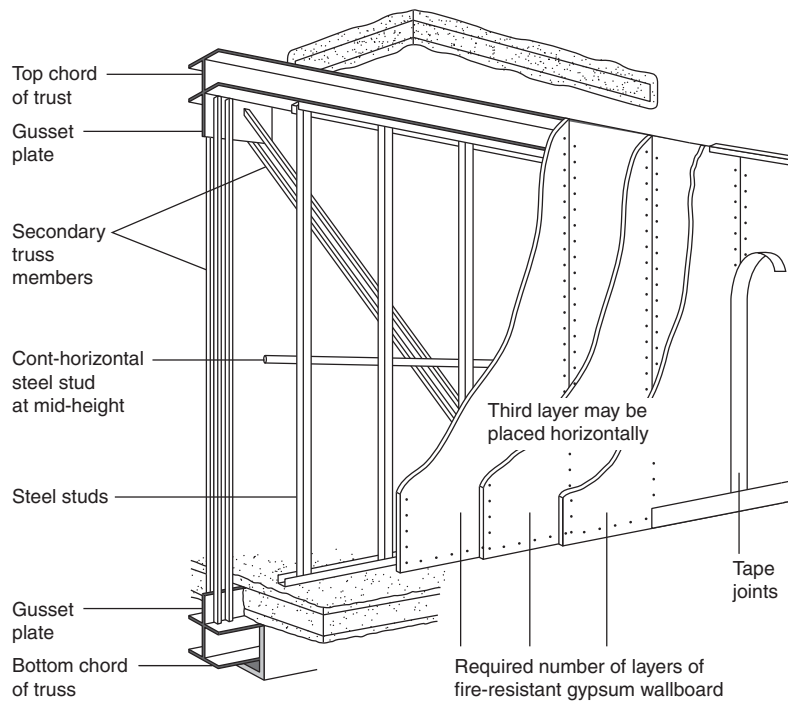


Figure 4-9.15. Staggered truss protection with envelope protection.<sup>33</sup>

## Heat Transfer Analyses

Heat transfer analyses are applied to determine the time period required to heat structural members to a specified critical temperature or to provide temperature data as input to the structural analysis of the heated member. The time required to heat the member to a specified critical temperature is often defined as the fire endurance time of the member.

The critical temperature of a structural member can be determined by referring to the temperature endpoint criteria cited in ASTM E119<sup>1</sup> or by a structural assessment, as is discussed later in this chapter.

The available types of heat transfer analyses can be grouped into the following categories:

1. Numerical methods
2. Graphical solutions
3. Computer programs

### Numerical Methods

Many numerical methods are available to estimate the temperature rise in steel structural elements. The equations are derived from simplified heat transfer approaches.

**Unprotected steel members:** The temperature in an unprotected steel member can be calculated using a quasi-steady-state, lumped heat capacity analysis. This method assumes that the steel member is at a uniform temperature. The equation for temperature rise during a short time period,  $\Delta t$ , is<sup>21</sup>

$$\Delta T_s = \frac{\alpha}{c_s(W/D)} (T_f - T_s) \Delta t \quad (2)$$

where

$\Delta T_s$  = temperature rise in steel (°F)(°C)

$\alpha$  = heat transfer coefficient from exposure to steel member (Btu/ft<sup>2</sup>·s·R)(W/m<sup>2</sup>·K),

$D$  = heat perimeter (ft)(m) (see Figure 4-9.16)

$c_s$  = steel specific heat (Btu/lb·°F)(J/kg·°C)

$W$  = steel weight per lineal foot (lb/ft)/(kg/m)

$T_f$  = fire temperature (R)(K)

$T_s$  = steel temperature (R)(K)

$\Delta t$  = time step (s)

where

$$\alpha = \alpha_r + \alpha_c$$

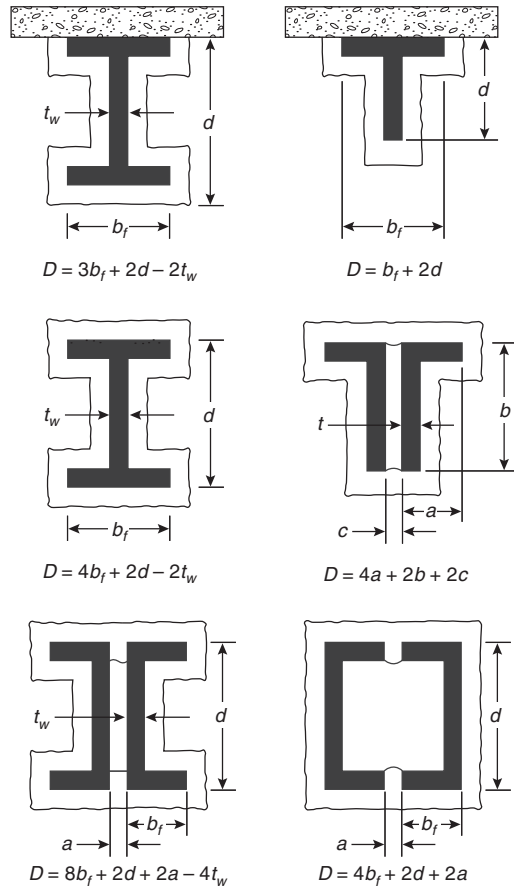
$\alpha_r$  = radiative portion of heat transfer

$$\alpha_r = \frac{C_1 \epsilon_f}{T_f - T_s} (T_f^4 - T_s^4)$$

where  $C_1 = 4.76 \times 10^{-13}$  Btu·s·ft<sup>2</sup>·R<sup>4</sup> ( $5.77 \times 10^{-8}$  W/m<sup>3</sup>·K<sup>4</sup>) and  $\epsilon_f$ , the effective emissivity, can be evaluated from Table 4.97.

$\alpha_c$  = convective portion of heat transfer

$$9.8 \times 10^{-4} \text{ to } 1.2 \times 10^{-3} \text{ Btu/ft}^2 \cdot \text{s} \text{ (20 to 25 W/m}^2 \cdot \text{K)}$$

Figure 4-9.16. Heated perimeter for steel truss shapes.<sup>33</sup>

The quasi-steady assumption dictates that the time step should be small, that is, on the order of 10 s.<sup>59</sup>

Equation 2 is successively applied up to the time duration of interest. Correlations for the time-temperature curve associated with standard fire resistance tests are included by Lie, in another chapter of this handbook. For the ISO 834 test,  $T_f$  at any time,  $t$ , can be estimated by the following expression:<sup>21</sup>

$$T_f = C_T \log_{10} (0.133t + 1) + T_0 \quad (3)$$

where

$$C_T = 620 \text{ with } T_f, T_0 \text{ in } ^\circ\text{F}$$

$$345 \text{ with } T_f, T_0 \text{ in } ^\circ\text{C}$$

**Protected steel members:** For protected members, the thermal resistance provided by the insulating material must be considered. If the thermal capacity of the insulation layer is neglected,<sup>21</sup>

$$\Delta T_s = \frac{k_i}{c_s h W/D} (T_f - T_s) \Delta t \quad (4)$$

where all parameters are as defined in Equation 2, and

Table 4-9.7 Effective Emissivity<sup>35</sup>

Type of Construction	Resultant Emissivity
1. Column exposed to fire on all sides	0.7
2. Column outside facade	0.3
3. Floor girder with floor slab of concrete, only the underside of the bottom flange being directly exposed to fire	0.5
4. Floor girder with floor slab on the top flange	
Girder of 1 section for which the width-depth ratio is not less than 0.5	0.5
Girder of 1 section for which the width-depth ratio is less than 0.5	0.7
Box girder and lattice girder	0.7

$k_i$  = thermal conductivity of insulation material (Btu/ft·s·°F) (W/m·°C)

$h$  = protection thickness (ft) (m)

Malhotra suggests that the thermal capacity of the insulation material may be neglected if the following inequality is true (see parameter definitions for Equation 2):<sup>21</sup>

$$c_s W/D > 2c_i \rho_i h$$

If the thermal capacity must be accounted for, as in the case of gypsum and concrete insulating materials, then

$$\Delta T_s = \frac{k_i}{h} \left[ \frac{T_f - T_s}{c_s (W/D) + 1/2c_i \rho_i h} \right] \Delta t \quad (5)$$

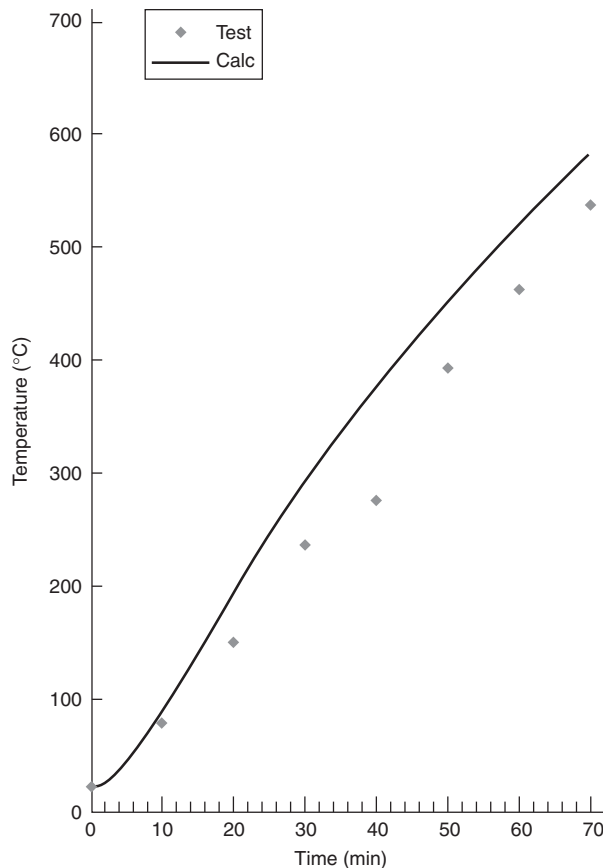
where all parameters are as defined for Equation 2, and  
 $c_i$  = specific heat of insulating material (Btu/lb·°F) (J/kg·°C)  
 $\rho_i$  = density of insulating material (lb/ft<sup>3</sup>) (kg/m<sup>3</sup>)

An evaluation of the predictive capability of the lumped heat capacity approach using Equation 5 for protected steel sections was conducted by Berger for steel columns protected with a spray-applied cementitious material.<sup>36</sup> The analysis consisted of comparing predicted versus measured temperatures for steel columns exposed to the standard fire exposure. A comparison of the predicted versus measured times for the steel column to reach 538°C is provided in Table 4-9.8. A comparison of the predicted temperature with that measured for one protected steel column assembly is provided in Figure 4-9.17.

Predictions of temperature rise in steel beams by the lumped heat capacity approach are prone to be inherently less accurate than those for steel columns.<sup>37</sup> As noted previously, a steel beam in contact with a slab only has three sides exposed to a fire and also will lose heat to the slab.<sup>38</sup> Consequently, the temperature of a steel beam exposed to fire is likely to vary appreciably from the bottom flange to the top flange, stretching the validity of the uniform temperature assumption. Nonetheless, for many engineering applications, the lumped heat capacity approach can provide a conservative estimate of the average temperature

**Table 4-9.8 Comparison of Predicted Time from Lumped Heat Capacity Analysis and Measurements for Protected Steel Column to Reach 538°C**

Shape	<i>h</i> (cm)	Test (min)	Calc. (min)
W 6 × 16	1.9	58	56
	3.8	112	119
	7.6	210	251
W 8 × 28	3.5	122	121
	8.3	291	298
	9.5	355	352
W 10 × 49	1.9	70	62
	5.6	217	220
W 12 × 106	3.8	200	203
W 14 × 228	1.4	123	140
W 14 × 233	2.9	225	251



**Figure 4-9.17. Predicted steel column temperature.<sup>36</sup>**

rise of a steel beam.<sup>39</sup> Heat losses to the slab may be compensated for by reducing the effective flame emissivity to 0.5.<sup>35</sup> However, if the temperature gradient across the beam is important, another analytical approach will need to be applied.<sup>37</sup>

**Exterior steel columns and steel spandrel beams:** A design guide is available for calculating the exposure of exterior steel columns and steel spandrel beams.<sup>40</sup> The guide is based on research by Law and basic radiation heat transfer principles.<sup>41</sup> A similar calculation procedure is available in the Eurocodes.<sup>9</sup>

The temperature of the steel member is calculated from a steady-state conduction analysis. The exposure boundary conditions consist of radiant heating from a fully developed room fire and flames emitting from windows near the steel member. For this method, a specific design is considered unacceptable if the steel temperature exceeds 1000°F.

**Liquid-filled columns:** The design calculations for liquid-filled columns are based on the thermal capacity of the liquid. The design of a liquid-filled column fire protection system consists of three major steps:

1. Heat transfer analysis
2. Determination of volume of liquid required
3. Pipe network design

The heat transfer analysis is used to assess the impact of fire exposure on the liquid-filled column. The heat transfer analysis considers radiation and convection heat transfer from the fire to the column surface, conduction through the column wall, and convection with localized boiling into the liquid. Both temperature of the steel column and total amount of heat transferred to the liquid causing evaporation are determined as a result of this analysis.

The liquid volume calculation is important to ensure the column remains full of liquid for the entire fire exposure period. Since heat transferred to the liquid will cause some evaporation, a supplemental amount of liquid must be provided in a storage tank.

The final step in the design method is a hydraulic analysis of the tubular column and pipe network. This analysis assesses the ability of the liquid to circulate based on friction losses, elevation changes, and buoyancy of the heated liquid.

A comprehensive design aid for liquid-filled columns is available.<sup>42</sup> Since the procedure is rather lengthy, it will not be reviewed here.

### Graphical Solutions

Because heat transfer analyses can be very tedious and may involve the use of complex computer programs, graphic solutions have been formulated to simplify the estimation of steel temperature. Graphs of the temperature of protected steel members have been developed by Malhotra,<sup>21</sup> Jeanes,<sup>12</sup> Lie,<sup>15</sup> and others.

The series of graphs developed by Malhotra,<sup>21</sup> presented in Figure 4-9.18, for estimating the temperature of steel members exposed to the standard exposure are based on the lumped heat capacity approach described in the previous section. Steel temperatures are plotted versus the  $D/A$  ratio (analogous to the inverse of  $W/D$ ) for selected time periods of exposure and thermal resistances of the insulating material. Time periods of 30 to 120 min are noted in the graphs. The range of thermal resistances of the insulating material covered by these graphs is 0.01 to 0.30  $(W/m^2 \cdot ^\circ C)^{-1}$  (0.003 to 0.10)  $(Btu/ft^2 \cdot hr \cdot ^\circ F)^{-1}$ .

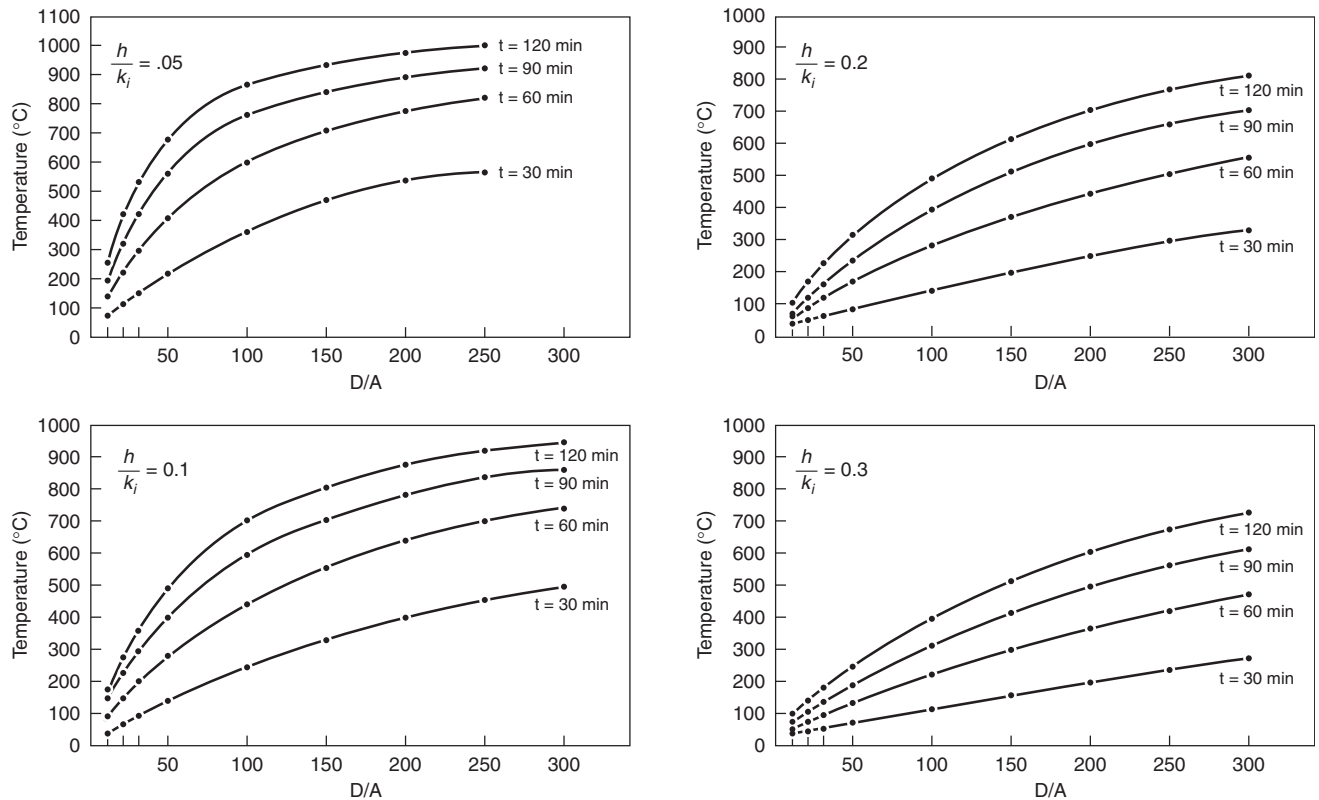


Figure 4-9.18. Relationship of heated area to steel weight with temperature.<sup>21</sup>

Based on the application of FIRES-T3, a heat transfer computer program which will be described in the next section, Jeanes formulated a series of time-temperature graphs of protected steel beams.<sup>12</sup> The steel beams are protected by a proprietary specific spray-applied cementitious material with a range of thicknesses of 0.5 to 1.5 in. (12.7 to 38.1 mm). Graphs are available for a variety of common wide-flange beam shapes.<sup>12</sup> Examples of these graphs are presented in Figure 4-9.19 with graphs addressing the average and single-point steel temperatures relating to the maximum endpoint criteria from ASTM E119.<sup>1</sup> Average and single-point steel temperatures are represented by the dashed lines. These graphs can be used to determine the thickness of protection material required to provide a desired level of fire resistance. Alternatively, the fire endurance can be estimated for a particular steel beam and insulation thickness design which has not been tested.<sup>12</sup>

Information from numerous applications of FIRES-T3 examining the time-temperature response of steel beams protected with a spray-applied cementitious material exposed to the standard fire exposure is summarized in Figure 4-9.20. Using this graph, the fire endurance of protected steel beams with a  $W/D$  ratio of 0.4 to 2.5 lb/ft-in. can be determined for thicknesses of the spray-applied protection between 1.3 to 3.8 cm (0.5 to 1.5 in.).

Lie provides graphical representations of the exact solutions of the governing differential equations for the temperature of protected steel members exposed to the

standard fire.<sup>15</sup> The heat transfer is assumed to be one-dimensional through the insulation layer. A uniform temperature throughout the steel cross section is assumed. The two graphs presented in Figure 4-9.21 are applicable to a wide range in the Fourier number,  $Fo$ , for the insulation layer. In order to use the graphs, the following dimensionless parameters must be defined:

$$Fo = \frac{at}{h^2}$$

$$N = \frac{\rho_i c_i h}{c_s (W/D)}$$

$$\theta = \frac{T - T_0}{T_m - T_0}$$

where

$a$  = thermal diffusivity of insulation (ft<sup>2</sup>/hr) (m<sup>2</sup>/hr)

$t$  = heating time (hr)

$h$  = thickness of insulation (ft) (m)

$\rho_i$  = density of insulation (lb/ft<sup>3</sup>) (kg/m<sup>3</sup>)

$c_i$  = specific heat of insulation (Btu/lb·°F)

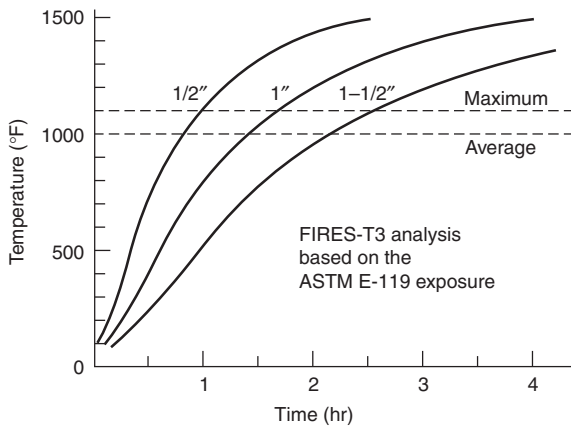
$c_s$  = specific heat of steel (Btu/lb·°F)

$T$  = temperature of steel at time  $t$  (°F) (°C)

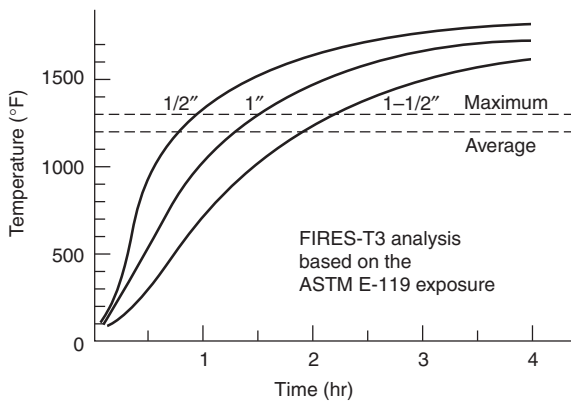
$T_0$  = initial temperature of steel (°F) (°C)

$T_m$  = mean fire temperature (°F) (°C)

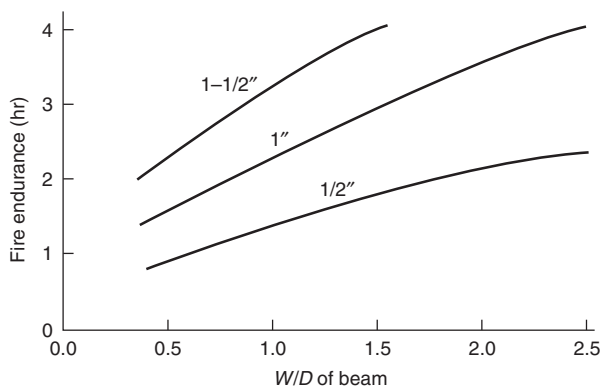
Average Section Temperature of Steel Beam,  
W12  $\times$  14 ( $W/D = 0.40$ ), for Various Thicknesses  
of Direct-Applied Fire Protection



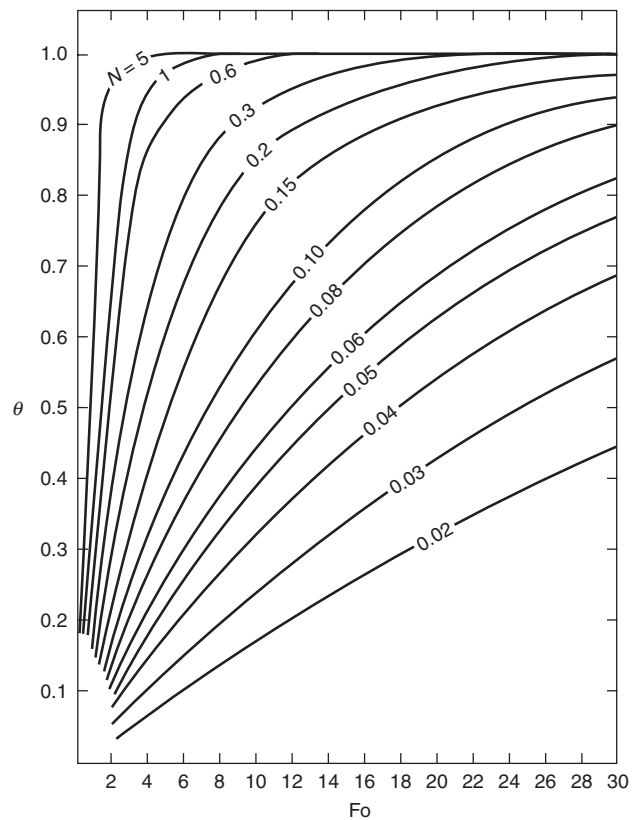
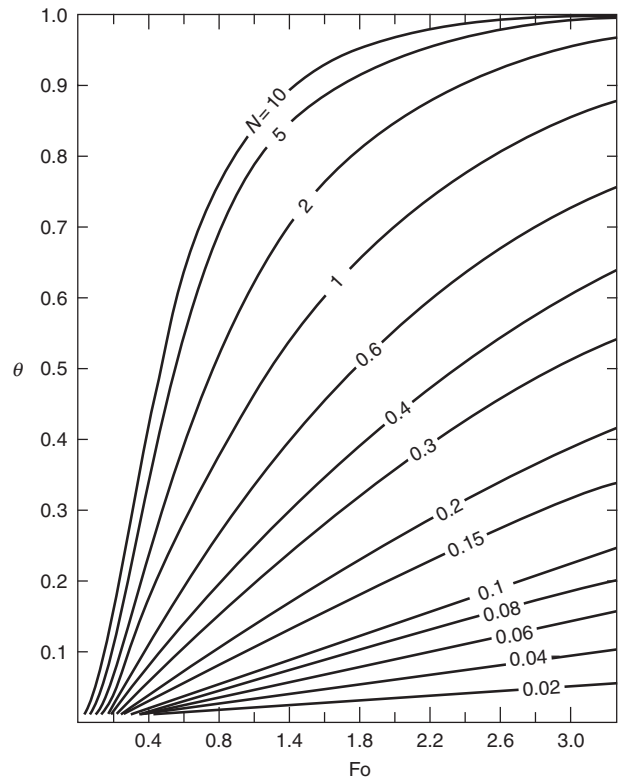
Maximum Steel Beam Temperature,  
W12  $\times$  14 ( $W/D = 0.40$ ), for Various Thicknesses  
of Direct-Applied Fire Protection



**Figure 4-9.19.** Predicted steel beam temperature by FIRES-T3.<sup>12</sup>



**Figure 4-9.20.** Fire endurance of steel beams versus fire protection thickness for average section temperature of 1000° F (538° C). (Based on FIRES-T3 analysis of ASTM E119 fire exposure.)<sup>12</sup>



**Figure 4-9.21.** Dimensionless steel temperature versus Fourier numbers.<sup>15</sup>



The mean fire temperature associated with a heating time,  $t$ , for these graphs is calculated from the standard time-temperature curve, where

$$T_m = \begin{cases} 150(\ln 480t - 1) - 30/t, & T^\circ\text{C} \\ 270(\ln 480t) - 238 - 54/t, & T^\circ\text{F} \end{cases}$$

**EXAMPLE 4:**

Determine the fire resistance of a  $W 24 \times 76$  steel beam based on the temperature endpoint criteria noted in ASTM E119. The beam is protected with 0.50 in. (12.7 mm) of spray-applied cementitious material, by three methods:

1. Graphical approach from Jeanes<sup>12</sup>
2. Graphical approach by Lie<sup>15</sup>
3. Quasi-steady-state approach by Malhotra<sup>21</sup>

**SOLUTION:**

A  $W 24 \times 76$  steel beam has a  $W/D$  ratio of 1.03 lb/ft-in. or 12.36 lb/ft<sup>2</sup>. The material properties are evaluated at mean temperatures expected during the exposure. The fire resistance can be assessed using the temperature endpoint criteria in ASTM E119. Mean temperatures of 500°F (260°C) and 750°F (400°C) are selected (arbitrarily) for the steel and insulation, respectively, to determine the thermal properties. The following material property values are assumed:<sup>12</sup>

	Steel	Insulation
Thermal conductivity (Btu/ft·hr·°F)	25.6	0.067
Specific heat (Btu/lb·°F)	0.132	0.304
Density (lb/ft <sup>3</sup> )	490	15

**Jeanes's graph:** Using Figure 4-9.21 with a  $W/D$  of 1.03 lb/ft-in. and an insulation thickness of 0.50 in. (12.7 mm), the fire endurance is estimated to be 1.33 hr or 80 min.

**Lie's graph:** Evaluating the dimensionless parameters,

$$Fo = \frac{at}{h^2}$$

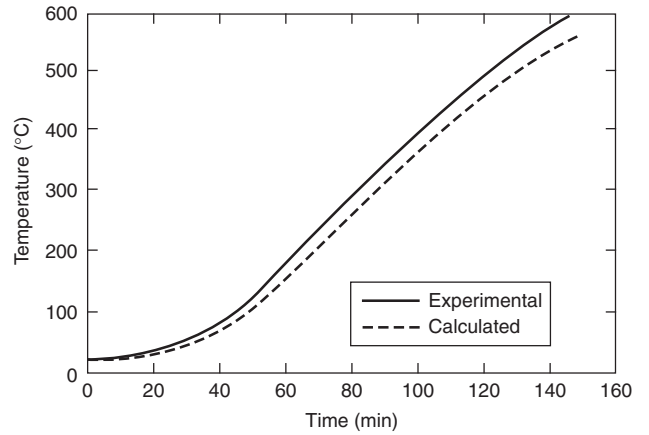
where

$$\alpha = \frac{k_i}{\rho_i c_i} = \frac{0.067}{15 \times 0.304} = 0.0147 \text{ ft}^2/\text{hr}$$

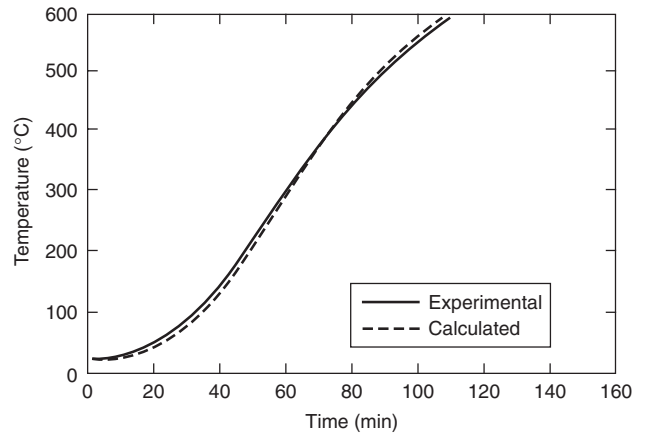
$$Fo = \frac{0.0147t}{(0.5/12)^2} = 8.47t \quad (t \text{ in hr})$$

Referring to Figure 4-9.22 and using a trial and error approach with a critical temperature selected as 1000°F (538°C), the fire endurance time is estimated as approximately 75 min.

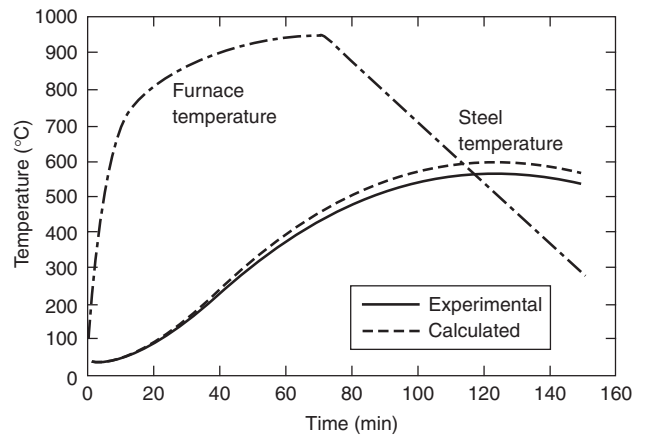
**Quasi-steady-state approach:** First, a check is performed to determine if the thermal capacity of the insulation material must be considered.



15 × 15 cm steel core, insulated by fire brick



20 × 20 cm steel core, insulated by heavy clay brick



20 × 20 cm steel core, insulated by vermiculite boards

**Figure 4-9.22. Comparison of calculated and measured steel temperatures.<sup>43</sup>**

$$c_s W/D > 2c_i \rho_i h$$

$$0.132 \times 12.36 > 2 \times 0.304 \times 15 \times 0.50/12$$

$$1.63 > 0.38$$

Disregarding the thermal capacity of the insulation, Equation 4 is used to predict the steel temperature rise for each time step.

$$\Delta T_s = \frac{0.067/3600}{0.0132 \times 0.50/12 \times 12.36} (T_f - T_s) \Delta t$$

$$= 2.74 \times 10^{-4} (T_f - T_s) \Delta t$$

Time	Steel Temperature (°C)	Fire Temperature (°C)	Fire-Steel Temperature (°C)	W/m <sup>2</sup> ·K k/h	ΔT <sub>s</sub> (°C)
10	20.0	46	26	9.13	0.1
20	20.1	72	51	9.13	0.2
30	20.3	96	76	9.13	0.3
40	20.5	120	99	9.13	0.3
50	20.8	143	122	9.13	0.4
3220	534.2	888	353	9.13	1.2
3230	535.3	888	353	9.13	1.2
3240	536.5	888	352	9.13	1.2
3250	537.7	889	351	9.13	1.2
3260	538.9	889	350	9.13	1.2
3270	540.1	890	350	9.13	1.2
3280	541.2	890	349	9.13	1.2

Thus, the fire endurance is 54 min.

The fire endurance calculated by the three methods can be compared as follows:

Jeanes (FIRES-T3)	80 min
Lie	75 min
Quasi-steady-state	54 min

The agreement between the fire endurance times determined by Jeanes's and Lie's graphs is very good. The significantly reduced fire endurance calculated using the quasi-steady-state approach is attributable to the approximate nature of the lumped heat capacity method assuming an adiabatic surface at the beam-slab interface.

### Computer-Based Analyses

Several computer-based analyses are available to estimate the temperature rise of steel members. The analyses range from a spreadsheet procedure to perform the iterative calculations for the quasi-steady-state approach to finite element models.

Spreadsheets are one example of providing a framework to perform the iterative, quasi-steady calculations.<sup>36,37,44</sup> Typically, the spreadsheet procedures mimic the quasi-steady analysis procedure described previously, including the evaluation of material properties at a mid-range temperature for the exposure of interest. Although temperature-dependent material properties can be included within the spreadsheet framework, the accuracy implied by considering temperature-dependent properties is not consistent with the first-order nature of the quasi-steady approach.

Another framework for conducting computer-based analyses includes the numerous mathematical-equation-solver software packages. This software can be used to

conduct the iterations associated with the quasi-steady approach or to solve the partial differential equations exactly.

Harmathy and Lie developed a two-dimensional finite difference model to predict the temperature rise in protected steel columns.<sup>43</sup> The two-dimensional network is formulated over the cross-section of the insulation layer, assuming the temperature to be independent of length. The steel is assumed to be a perfect conductor (i.e., the temperature is uniform throughout the steel). Heat transfer via radiation is considered across any air spaces enclosed by the insulation and steel.

The boundary conditions included by Harmathy are those associated with the ASTM E119 test.<sup>1</sup> To simplify the model, convection is disregarded, since convection comprises a minor portion of the heat transfer process in the furnace test. A flame emissivity of 0.9 is selected. A comparison between the calculated and experimental steel temperatures is presented in Figure 4-9.22. As is evident, the agreement is very good for three insulating materials.

Pettersson et al.<sup>35</sup> include a finite difference formulation to predict the temperature rise of steel beams protected with a suspended ceiling exposed to a specified fire. The formulation uses a one-dimensional approximation accounting for conduction through the suspended ceiling and floor slab (above the beam), and radiation and convection in the air space between the slab and beam. The temperature of the steel is assumed to be uniform. The assembly is divided into several elements as depicted in Figure 4-9.23.

A system of simultaneous equations is derived for the temperature rise in each of the assembly elements. A numerical integration technique such as Runge-Kutta is used to obtain the solution. A comparison of the calculated versus experimentally observed temperatures for a steel beam is presented in Figure 4-9.24.

General heat-transfer finite-element programs have been available for many years.<sup>45</sup> FIRES-T3, TASEF-2, SAFIR, and SUPER-TEMPCALC, among others, have been

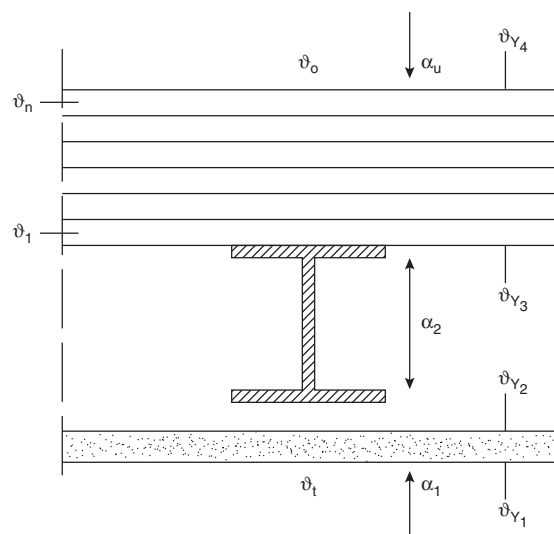
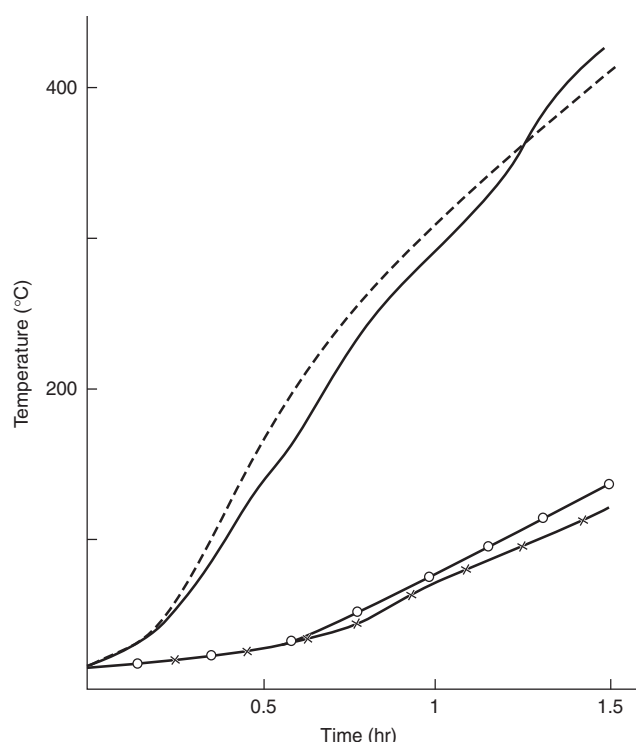


Figure 4-9.23. Division of the floor slab into elements.<sup>35</sup>



**Figure 4-9.24.** *Calculated (--) and measured (—) steel temperature-time ( $\theta_s - t$ ) curve for a floor girder IPE 140 with insulation in the form of a suspended ceiling of 40-mm-thick mineral wool slabs of density  $\gamma = 150 \text{ kg/m}^3$ . The figure also gives the calculated (—o—) and measured (—x—) temperature-time curve for the top of the 50-mm-thick concrete floor slab.<sup>35</sup>*

developed specifically to address the heating of assemblies with steel structural members exposed to fire conditions.<sup>46-48</sup>

TASEF-2 examines the conduction heat transfer through assemblies.<sup>46</sup> Assemblies may include internal voids, in which convection and radiation heat transfer modes are considered. Two time-temperature curves are available: (1) the ISO 834 standard time-temperature curve and (2) a time-temperature curve from a ventilation-controlled fire.

SUPER-TEMPCALC can also be used to analyze the conduction heat transfer through assemblies with air gaps. Numerous fire curves are included within the software.

FIRES-T3 was specifically developed to examine the heating of structural members exposed to fire conditions.<sup>47</sup> FIRES-T3 has been applied successfully to predict the temperature rise in protected steel beams and columns.<sup>12,49</sup> Almand used a finite-difference heat-transfer model to estimate the protection thickness of spray-applied cementitious material required for tubular steel columns.<sup>50</sup>

The input data requirements for the heat transfer computer models can be grouped into two categories:

1. A description of the assembly
2. A description of the fire exposure

The information necessary to describe the assembly includes geometric factors (dimensions, shape of member) and material property values (thermal conductivity, specific heat, and density). The fire exposure is characterized in terms of the temperature of the surrounding environment and appropriate heat transfer coefficients. The geometry of the assembly is established by formulating an element mesh for the assembly of interest. Required material property data consists of the density, specific heat, and thermal conductivity of the steel and insulation. Material property data is available for a limited number of insulation materials.<sup>12,51</sup> The exposure associated with the ASTM E119 test<sup>1</sup> may be selected as the fire exposure to be simulated by FIRES-T3.<sup>12,49</sup> A pre-processor routine for FIRES-T3 was recently developed by Stubblefield and Edwards.<sup>52</sup> TASEF and SUPER-TEMPCALC also includes a post-processor to generate graphs of the output.

For models using an explicit transient solution technique, such as FIRES-T3, caution must be exercised in selecting the time step and mesh size to obtain correct results that are numerically stable. TASEF-2 internally determines a numerically stable time step. Most heat transfer models do not address the effects of phase changes or chemical reactions that may influence the heating process. Phase changes and chemical reactions have been accounted for by altering the value of the material properties. Milke addressed the evaporation of free water in a spray-applied cementitious material by increasing the specific heat in a narrow temperature region around 100°C (212°F).<sup>49</sup>

Agreement between the predicted and experimental average steel temperatures is quite good in both applications of FIRES-T3 by Jeanes and Milke. A comparison of the temperature history for a steel column protected with a spray-applied cementitious material subjected to the ASTM E119 test is presented in Figure 4-9.25. A similar comparison is presented in Figure 4-9.26 for steel beams protected with the same material.<sup>12</sup>

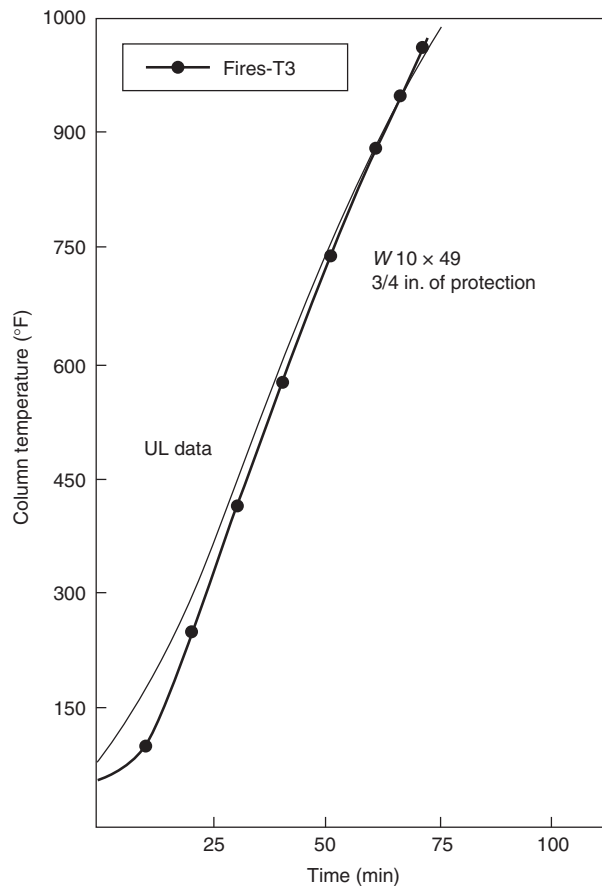
FIRES-T3 has also been used to conduct a preliminary analysis of the heating of partially protected steel columns (i.e., where a portion of the spray-applied protection is missing).<sup>53</sup> The analysis indicated that even a small portion of missing protection significantly decreased the fire resistance of the column, especially for cases involving small columns. Results of the analysis are indicated in Figure 4-9.27.

## Structural Analyses

The structural analysis methods calculate one of three parameters: deflection, critical temperature, or critical load. In several of the methods, all three of the parameters may be considered, since they are interrelated. Algebraic equations, graphs, and computer programs are available to perform a structural analysis for the purpose of addressing fire resistance.

### General Discussion of Three Parameters Addressed in Structural Analysis

**Deflection:** The total deflection and rate of deflection can be calculated for loaded and heated steel beams by

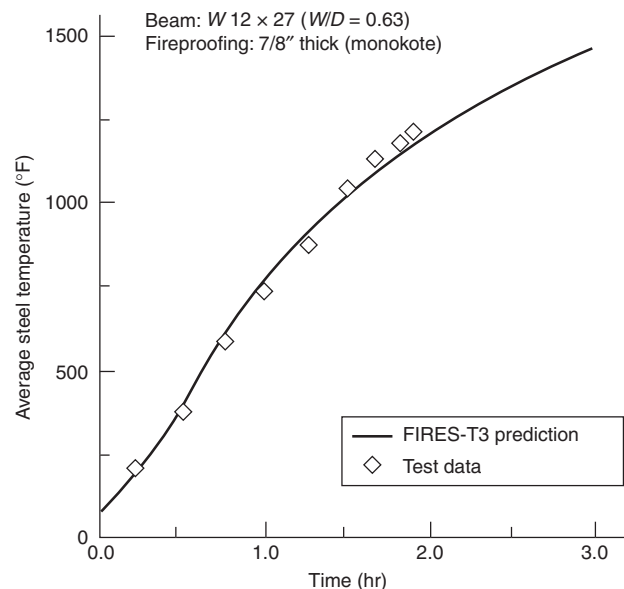
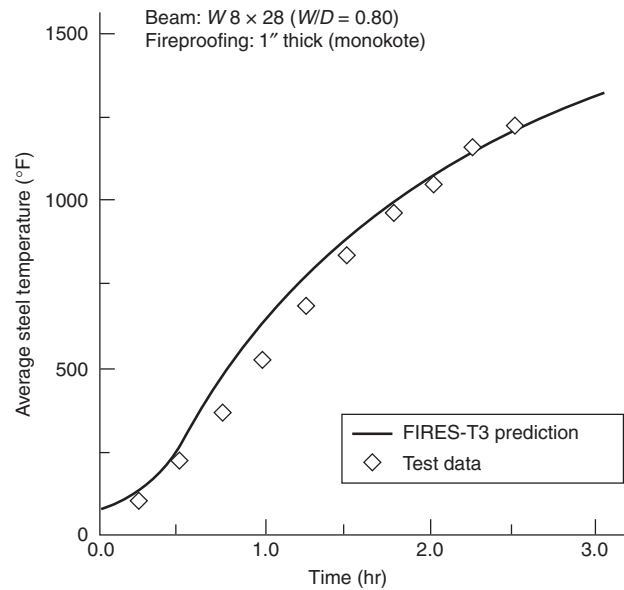


**Figure 4-9.25. Comparison of predicted and measured average steel column temperature.<sup>47</sup>**

considering all sources of strain. The total strain comprises components of the elastic and plastic strains due to the applied loads, thermal strain (due to thermal expansion), and creep strain.

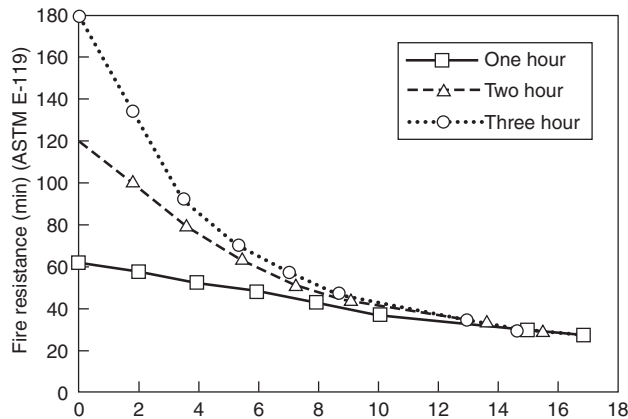
The calculated deflection and rate of deflection can be compared with established maximum limits of each. The Robertson-Ryan criteria have been widely accepted for this purpose.<sup>20,54,55</sup> However, calculation of the deflection of unheated beams is difficult except for simple loadings, geometries, and end conditions. Adding the thermal expansion and creep components further complicates the calculation, virtually requiring computer solution.

**Critical temperature:** As mentioned earlier in the chapter, the material properties of steel change with increasing temperature. The most important material properties for critical-temperature calculations are yield strength, ultimate strength, and modulus of elasticity. The critical temperature is defined as the temperature at which the material properties have decreased to the extent that the steel structural member is no longer capable of carrying a specified load or stress level. In this context, the factor of safety of the member is considered to be reduced if the



**Figure 4-9.26. Comparison of experimental data and FIRES-T3 analysis.<sup>12</sup>**

member reaches unacceptable stress levels, buckling becomes imminent, or deflections exceed maximum limits. The critical temperature can be calculated as long as the dependence of the material properties with temperature is known. There are numerous algebraic equations to calculate the critical temperature of steel structural members.<sup>56</sup> Often, the critical temperature is defined based on temperature limits stated in the standard test. However, in recent tests steel members experienced temperatures in excess of 800°C (1470°F) without collapse.<sup>57</sup>



**Figure 4-9.27.** Fire resistance versus percent protection loss for W 10 × 49 column, flange exposure.

**Critical load:** The critical load is defined as the minimum applied load that will result in failure if the structural member is heated to a temperature,  $T$ . The critical load can be expressed as a point load or distributed load. As with critical temperature, the critical load calculation requires the material properties at elevated temperatures. Critical load calculations can be conducted with algebraic equations or with a computer program.

## Algebraic Equations: Critical Temperature

### Beams

The critical temperature of Grade 250 steel beams with an allowable stress of 20,000 psi (138 MPa) can be determined using equations by Lie and Stanzak.<sup>30</sup> The Lie and Stanzak equations account for creep strain and assume the beam is simply supported and thermally unrestrained.

Similar approaches have been developed by Malhotra,<sup>21</sup> Vinnakota,<sup>55</sup> and Kruppa.<sup>58</sup> Differences in the percent reduction in yield stress or modulus of elasticity are related to design method (elastic or plastic), factor of safety, and end conditions. Equations for the ratio of yield stress at elevated temperature with yield stress at ordinary room temperature are presented in Table 4-9.9. Typical values of  $Z_e/S$  are between 1.13 and 1.15 for I sections,<sup>21</sup> and 1.5 for rectangular sections.

Another example of the second approach is the analysis of the critical temperature of beams by European Convention for Constructional Steelwork (ECCS).<sup>56,59</sup> The ECCS guide addresses the maximum allowable reduction in yield strength by considering the applied loading, beam geometry, structural end conditions, and whether the applied loading results in stresses in the elastic or plastic range. Critical temperature calculations based on the ECCS analysis are presented in Table 4-9.10.

#### EXAMPLE 5:

Determine the critical temperature of a simply supported W 12 × 26 steel beam supporting a 53-in.- (1.35-m-)

**Table 4-9.9 Critical Stress Equations<sup>21</sup>**

Design Basics	Critical Yield Stress
Elastic design	$\frac{\sigma_{YT}}{\sigma_Y} = \frac{1}{F_e} \frac{Z_e}{Z_p}$
Plastic design	$\frac{\sigma_{YT}}{\sigma_Y} = \frac{1}{F_p}$

where

$\sigma_{YT}$  = critical yield stress at elevated temperature,  $T$

$\sigma_Y$  = yield stress at ordinary room temperature

$F_e$  = factor of safety, elastic design

$F_p$  = factor of safety, plastic design

$Z_e$  = elastic section modulus

$Z_p$  = plastic section modulus

thick rectangular slab. The applied moment is 41,750 ft·lb (15,480 N·m). The rectangular slab is 8 ft (2.4 m) wide. The section properties of the beam are

$$Z_e = 33.4 \text{ in.}^3 (547 \times 10^3 \text{ mm}^3)$$

$$I = 204 \text{ in.}^4 (84.9 \times 10^6 \text{ mm}^4)$$

Assume  $\sigma_y = 36,000$  psi (248 MPa).

**SOLUTION:**

Using Lie and Stanzak's equation for a beam,

$$T_{cr} = \frac{70,000}{45.62 - 4.23(I_d/T)} - 460$$

$$I_d = \frac{3^3 \times 96}{12} = 216 \text{ in.}^4$$

$$T = \frac{70,000}{45.62 - 4.23(216/204)} - 460 = 1,240^\circ\text{F}$$

**Columns.** Lie and Stanzak calculated a critical temperature of 941°F (505°C) for slender, axially loaded columns.<sup>30</sup> The calculation was based on the temperature for the onset of elastic buckling for columns under maximum permissible applied stress conditions.

The Euler buckling stress at which elastic buckling is imminent is given by

$$\sigma_{cr} = \frac{\pi^2 E_T}{\lambda^2} \quad (6)$$

where

$\sigma_{cr}$  = Euler buckling stress (MPa) (psi)

$E_T$  = modulus of elasticity at temperature  $T$  (MPa) (psi)

$\lambda$  = slenderness ratio =  $Kl/r$


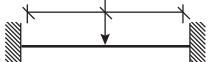
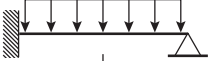
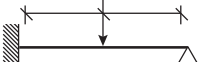
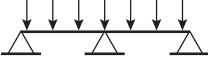
$r$  = radius of gyration (ft)(m)

$Kl$  = effective length of column (ft)(m)

Included in the ECCS guide<sup>59</sup> are dimensionless buckling curves for steel columns at elevated temperatures. These curves are presented in Figure 4-9.28.



Table 4-9.10 Critical Temperature of Steel Beams<sup>37</sup>

			factor $\frac{kq^*}{q_e}$ resp. $\frac{kq^*}{q_p}$				
Static System			0.3	0.4	0.5	0.6	0.7
Base of structural design at room temperature	Theory of plasticity	Statically determinate	585	540	490	430	360
		Statically indeterminate					
	Theory of elasticity	Statically determinate	605	565	525	475	425
		Statically indeterminate					
		$\Theta = 1.33$ 	640	605	575	545	510
		$\Theta = 1.0$ 	605	565	525	475	425
		$\Theta = 1.47$ 	650	615	590	560	535
		$\Theta = 1.12$ 	615	580	545	505	465
		$\Theta = 1.47$ 	650	615	590	560	535

$q_p$  = Ultimate plastic load  
 $q^*$  = Applied load  
 $k$  = Load multiplier  
 $\Theta$  = Factor addressing plastic reserve of beam from redistribution of moments.

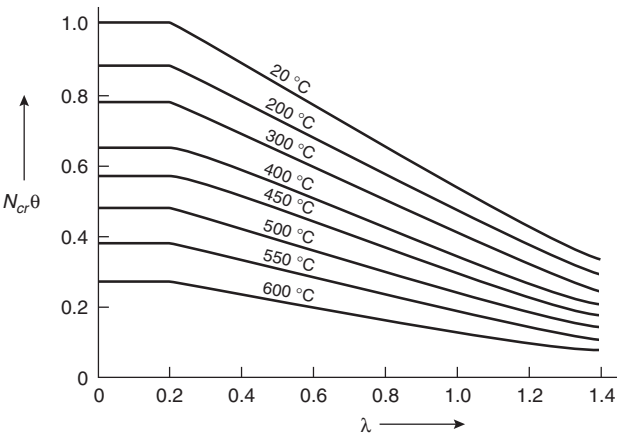


Figure 4-9.28. Dimensionless buckling curves for steel columns.<sup>59</sup>

Equation 6 is only valid for columns that buckle in the elastic range. Generally, slender columns having a slenderness ratio in excess of approximately 90 can be expected to buckle elastically. Buckling stresses for stout columns (slenderness ratio less than 90) are in the plastic range, requiring a more complex analysis. The failure mode for columns with a slenderness ratio between 80 and 100 cannot be reliably predicted.<sup>60</sup> The tangent mod-

ulus can be used instead of the modulus of elasticity in Equation 6 for stout columns. However, predictions of the critical temperature using Equation 6 may not be accurate, due to residual stresses from the steel fabrication process.<sup>60</sup> Thus, for stout columns, a conservative estimate for the critical temperature of steel columns may be obtained by determining the temperature at which the yield stress is equal to the applied stress.

General

Malhotra has observed that critical temperatures determined from the structural analysis algebraic equations will be somewhat low when compared to experimental data.<sup>21</sup> Thus, the following correction factors,  $V$ , are suggested by Malhotra to improve the prediction capabilities of the approach:

- 1. Columns:  $V = 0.85$
- 2. Statically determinate beams:  $V = 0.77 + 0.15 \frac{P_s}{P_u}$
- 3. Statically indeterminate beams:  $V = 0.25 + 0.77 \frac{P_s}{P_u}$

where

$P_s$  = service (applied) load (N or N/m) (lb or lb/ft)  
 $P_u$  = load to induce ultimate stress at midspan (N or N/m) (lb or lb/ft)

**EXAMPLE 6:**

Determine if the following steel column is expected to buckle if it achieves an average temperature of 1100°F (593°C). The column is simply supported, 15 ft (4.6 m) long and has an applied load of 12,000 psi (82.8 MPa). Assume the yield stress is 36,000 psi (248.4 MPa) and the modulus of elasticity is 30,000,000 psi. The characteristics of the column are

$$A = 8.23 \text{ in.}^2 \text{ (5310 mm}^2\text{)}$$

$$I = 21.6 \text{ in.}^4 \text{ (8.99} \times 10^6 \text{ mm}^4\text{)}$$

$$KL = 180 \text{ in. (4572 mm)}$$

At 1100°F (593°C):

$$E_T = 1 + \frac{T}{2000 \ln(T/1100)}$$

$$E_o = 15.6 \times 10^6$$

**SOLUTION:**

Calculate the slenderness ratio to determine the failure mode.

$$\lambda = \frac{KL}{r} = 110$$

Since the slenderness ratio exceeds 90, the column is susceptible to buckling. The buckling stress at 1100°F (593°C) is 12,700 psi (87.6 MPa). Thus, the column does not buckle due to the applied load and elevated temperature.

**Critical Stress**

**Columns:** Sample expressions for determining the critical stress for steel columns<sup>30</sup> are noted below.

$$P_{cr}^2 - P_{cr} \left[ \sigma_{yT} + \pi^2 E_T \left( 4.8 \times 10^{-5} + \frac{1}{\lambda^2} \right) \right] + \sigma_{yT} A \frac{\pi^2 E_T}{\lambda^2} = 0$$

where

$P_{cr}$  = critical point load (N) (lb)

$\sigma_{yT}$  = yield stress at temperature  $T$  (Pa) (psi)

$E_T$  = modulus of elasticity at temperature  $T$  (Pa) (psi)

$$\lambda = KL/r$$

In order to improve the prediction capabilities of the critical stress approach for slender columns, the modulus of elasticity should be replaced by the reduced modulus of elasticity.<sup>15</sup> The reduced modulus is defined as

$$E_r = \frac{4EE_T}{(\sqrt{E} + \sqrt{E_T})^2}$$

where

$E_r$  = tangent modulus

In addition, the 0.2 percent proof stress may be replaced by the 0.5 percent proof stress in the yield stress parameter.<sup>61</sup>

Results of a buckling analysis on concrete-filled square hollow sections are provided in Figure 4-9.29.

**Beams:** The expressions for the critical loads for beams assume at failure that the beam is in a state of full plasticity at the location of the maximum moment.<sup>61</sup> Obviously, in order to calculate the critical stress, the material property-temperature relationships must be known.

The critical distributed load for a simply supported beam is<sup>55</sup>

$$q_{cr} = \frac{8\sigma_{yT}Z_P}{L^2}$$

where

$q_{cr}$  = critical distributed load (N/m) (lb/ft)

$Z_P$  = plastic section modulus (m<sup>3</sup>) (in.<sup>3</sup>)

$L$  = span of beam (m) (ft)

$\sigma_{yT}$  = yield stress at elevated temperature (MPa) (psi)

Considering a cantilever beam with a point load applied one-third of the span from the fixed end, plastic hinges can be expected at the point of load application and at the fixed end. The critical load can be determined by

$$P_{cr} = \frac{7.5\sigma_{yT}Z}{L}$$

The above equations in this section do not account for creep strain. Based on an analysis of the deflection history of heated, loaded beams, Pettersson et al. include a load ratio,  $\beta$ , to determine the critical distributed stress.<sup>35</sup>

$$q_{cr} = \beta \frac{8\sigma_{yT}Z}{L^2}$$

where the yield stress is evaluated at ordinary room temperature, relaxing the need to know the yield stress-temperature relations.  $\beta$  is defined as the ratio of the load causing a maximum allowable deflection under fire conditions to the load inducing stresses equal to the yield stress at ordinary room temperature. Thus, the parameter  $\beta$  takes into account the dependence of both the yield stress and creep on temperature. Graphs of  $\beta$  are available for a variety of thermal restraint and structural end conditions.

The Eurocodes include a method of analysis using algebraic equations to consider the moment capacity of steel beams which have a temperature gradient through the depth of the beam.<sup>9</sup> The method involves dividing the beam into small isothermal sections and treating these isothermal sections as a composite beam (see Figure 4-9.30). In this case, the moment capacity of the beam is given as

$$M_{cap} = \sum_{i=1}^n \sigma_i A_i z_i$$

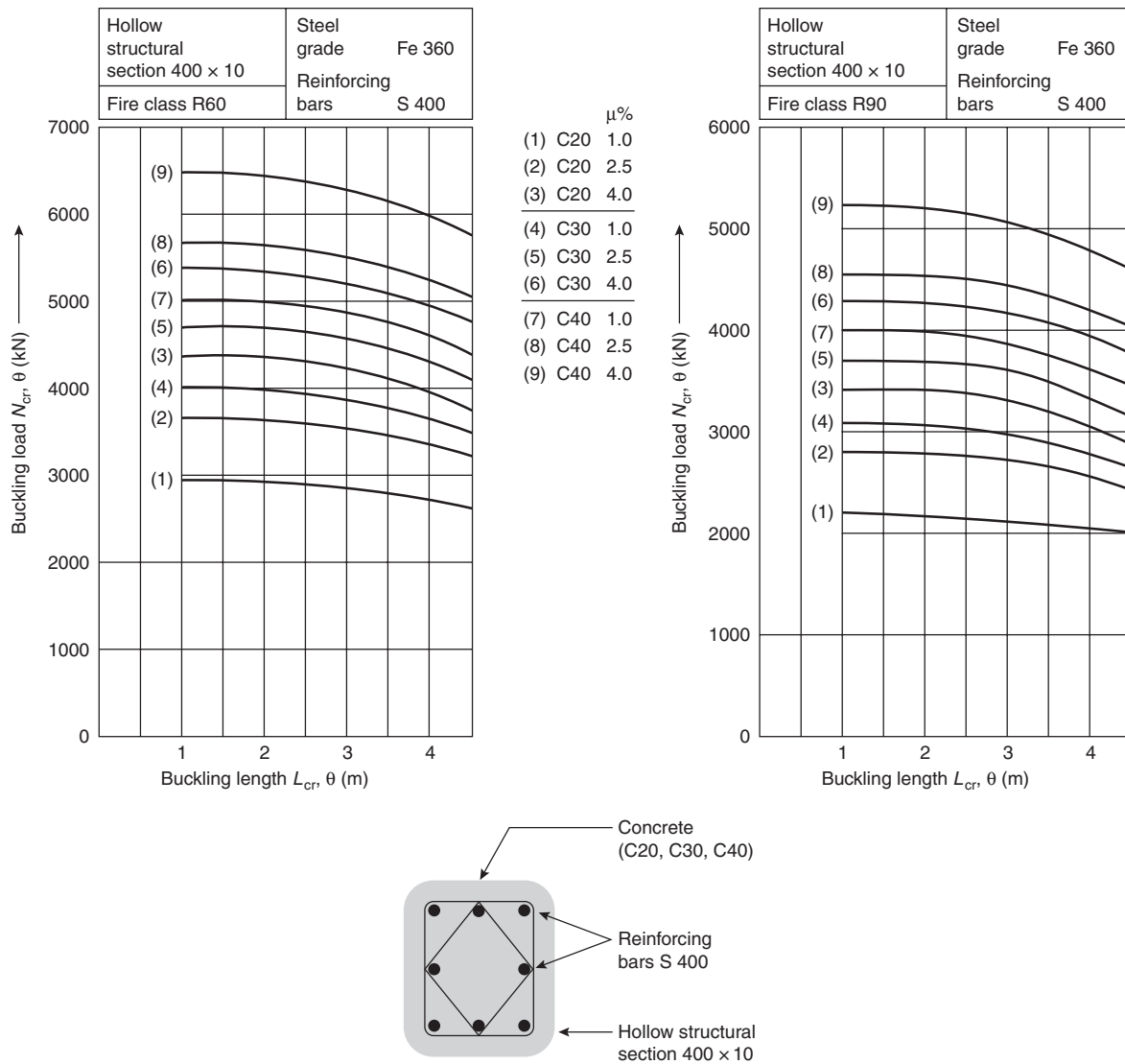
where

$M_{cap}$  = moment capacity (N·m) (lb·ft)

$\sigma_i$  = applied stress in isothermal element (Pa) (psi)

$A_i$  = area of isothermal element (m<sup>2</sup>) (ft<sup>2</sup>)

$z_i$  = distance from neutral axis to centroid of isothermal element (m) (ft)

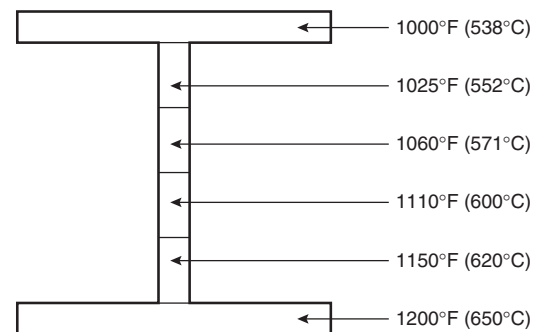


**Figure 4-9.29.** Design graphs for ISO fire resistance requirements R60 and R90. For the concrete-filled square hollow structural section 400 × 10, the axial buckling load is a function of the buckling length, of the concrete quality, and of the percentage  $\mu$  of reinforcement; this design diagram is based on a simple calculation model.<sup>8</sup>

### Computer Programs

Several finite element computer models are available to assess the structural response of fire-exposed structural members or frames. Sullivan et al. indicate that most of the existing finite element models used for structural fire protection analyses were developed originally for research applications.<sup>62</sup>

FASBUS-II is an example of a finite element model developed in the United States to evaluate the structural response of complex building assemblies such as floor assemblies consisting of a two-way concrete slab, steel deck, and steel beam.<sup>63</sup> Input for FASBUS-II includes the temperature distribution, temperature-dependent mechanical properties, geometry, end conditions, and loading. The output of FASBUS-II includes deflections, rotations,



**Figure 4-9.30.** Isothermal sections of beam.

and stresses in the components of the assembly, which then need to be compared to performance limits.

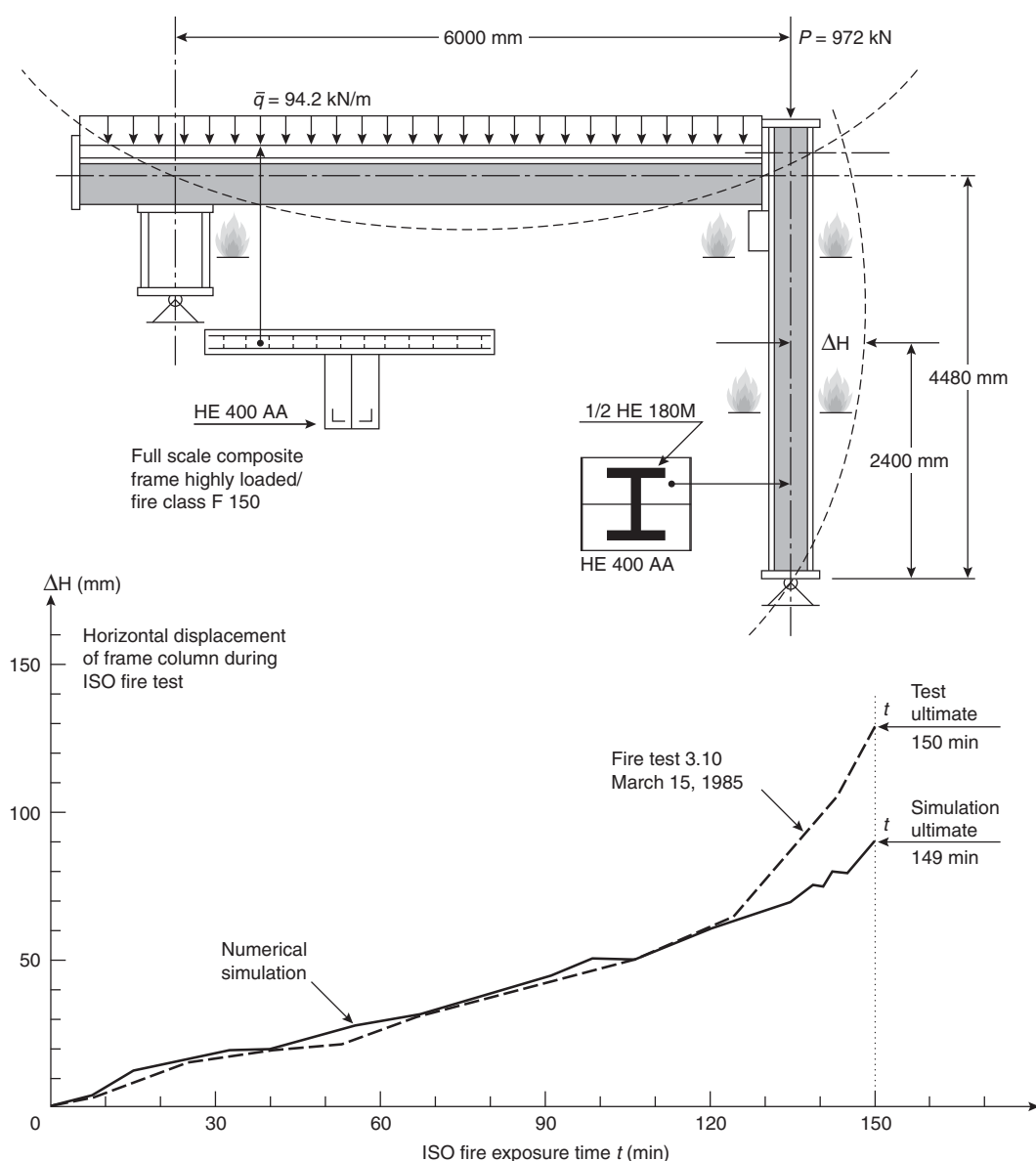
Sullivan et al. and Franssen et al. provide extensive reviews and comparisons of existing finite element models for structural fire protection applications.<sup>62,64</sup> According to Sullivan et al. all of the models make the following assumptions:

- Plane sections remain plane (Navier-Bernoulli hypothesis).
- Perfect composite action is assumed for steel-concrete assemblies, disregarding any slippage between the steel and concrete.
- Torsion is disregarded.
- Moisture effects are disregarded.
- Large displacements are not accurately modeled.

Traditionally, analysis of the response of the structure exposed to fire has been limited to an analysis of the response of single members. However, in structural frames comprising many members, load transfer or membrane action may occur to permit the steel member to maintain its integrity, despite achieving a temperature in excess of that typically associated with failure.

Load transfer allows stronger members to support additional loads not capable of being carried by heated, weak members. In order to capture this phenomenon, a frame analysis is required.<sup>44</sup> Numerous software packages are available to conduct the frame analysis. Results of a frame analysis are presented in Figures 4-9.31 and 4-9.32.

The frame analyses range from algebraic-equation-based methods to finite element analyses. Pettersson et al.



**Figure 4-9.31. Deformations measured and calculated by a numerical model for a composite frame.<sup>8</sup>**

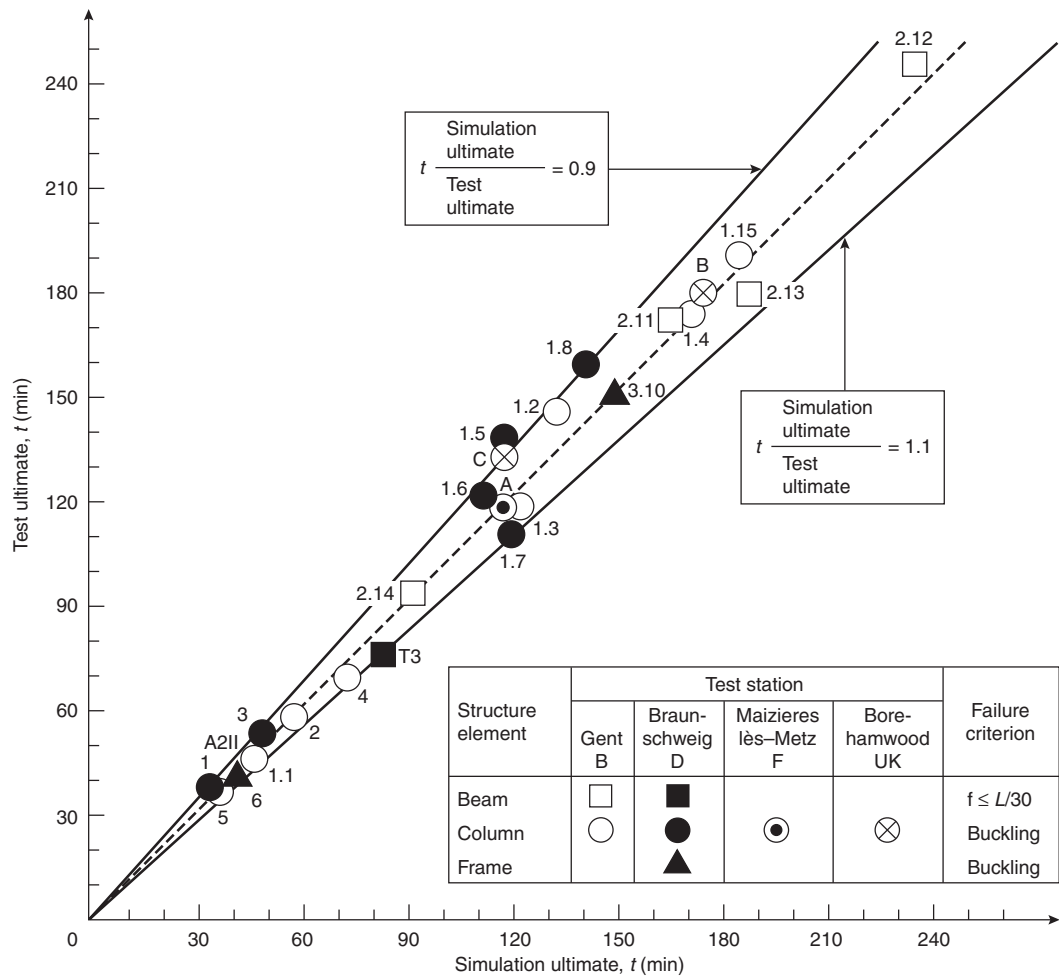


Figure 4-9.32. Fire resistance times measured and calculated by a numerical model for columns, beams, or frames of any cross section types (bare steel, protected steel, composite).<sup>6</sup>

include a frame analysis via algebraic equations used to determine displacement.<sup>35</sup> The frames consist of beams supported by one or two columns at mid-span. The analysis assumes that each beam or column has a uniform temperature (though the temperature of the beam is not required to be that of a column). A pinned connection between the structural members is assumed. The analysis considers the compatibility of the deformation of each member by requiring that the change in length of the column is equal to the beam deflection at the point of contact. Schleich et al. describe the application of CEFICOSS for a frame analysis.<sup>65,66</sup> The frame consists of a single beam and column, where one end of the column is connected to an end of the beam. Reasonable agreement is indicated between predicted and measured results. El-Rimavi et al. describe the application of another finite element model, NARR2, for the evaluation of a large building frame involving numerous beams and columns.<sup>67</sup> The large frame is divided into several subframes for computational ease. Good agreement is noted

between predictions of deflections and force resultants obtained involving simulations of the full building frame and subframes. Slightly greater failure temperatures were determined for semi-rigid connections as compared to rigid connections.

Nomenclature

- $a$  characteristic dimension
- $A$  cross-section area of steel tube, steel column
- $A_s$  cross-section area of steel column
- $b$  characteristic dimension
- $b_f$  width of flange
- $c$  characteristic dimension
- $c_c$  specific heat of concrete
- $c_i$  specific heat of protection material
- $c_s$  specific heat of steel
- $C_1$  constant



$C_2$	constant
$d$	outer diameter of steel pipe
$d$	depth of section
$D$	heated perimeter of steel section
$E_0$	modulus of elasticity at ambient temperature
$E_r$	reduced modulus
$E_t$	tangent modulus
$E_T$	modulus of elasticity at temperature $T$
$F$	factor of safety
$F_e$	factor of safety, elastic design
$F_p$	factor of safety, plastic design
$ Fo$	Fourier number
$h$	thickness of protection material
$H$	thermal capacity of steel section at ambient temperature
$k$	thermal conductivity of steel
$k_c$	thermal conductivity of concrete
$k_i$	thermal conductivity of protection material
$K$	end condition factor
$l$	unsupported length of column
$L$	inside dimension of one side of square concrete box protection
$L$	span of beam
$m$	moisture concrete of concrete
$N$	ratio of thermal capacity of protection material to that of steel
$P$	perimeter of steel tube
$P_{cr}$	critical point load
$P_s$	service (applied) load
$P_u$	ultimate load
$q_{cr}$	critical distributed load
$r$	radius of gyration
$R$	fire resistance
$R_0$	fire resistance with zero moisture content of concrete
$t$	wall thickness of steel pipe
$t$	time
$t_w$	width of web
$\Delta t$	time step
$T$	steel temperature
$T_f$	fire temperature
$T_m$	mean fire temperature
$T_0$	ambient temperature
$T_s$	steel temperature
$\Delta T_s$	change in steel temperature
$V$	correction factor
$W$	weight of steel section per unit length
$Z_e$	elastic section modulus
$Z_p$	plastic section modulus

### Greek

$\alpha$	thermal diffusivity (when used with Fourier number)
$\alpha$	heat transfer coefficient

$\alpha_c$	convective heat transfer coefficient
$\alpha_r$	radiative heat transfer coefficient
$\alpha_T$	coefficient of thermal expansion at temperature $T$
$\beta$	ratio of distributed load causing maximum allowable deflection to distributed load inducing yielding
$\epsilon_f$	fire emissivity
$\lambda$	slenderness ratio
$\theta$	dimensionless temperature
$\rho$	density
$\rho_i$	density of insulation material
$\sigma_{cr}$	critical stress for buckling
$\sigma_{y0}$	yield strength at ambient temperature
$\sigma_{yT}$	yield strength at temperature $T$

### References Cited

1. ASTM-119-98, *Standard Test Methods for Fire Tests of Building Construction and Materials*, American Society for Testing and Materials, Philadelphia (1998).
2. L.G. Seigel, "Fire Test of an Exterior Exposed Steel Spandrel," *Mtls. Res. and Standards*, 10, 2, pp. 10-13 (1970).
3. *Fire Resistance Directory*, Underwriters Laboratories, Northbrook, IL (2000).
4. R.W. Bletzacker, *Effect of Structural Restraint on the Fire Resistance of Protected Steel Beam Floor and Roof Assemblies*, Ohio State University, Columbus, OH (1966).
5. NFPA 251, *Standard Methods of Fire Tests of Building Construction and Materials*, National Fire Protection Association, Quincy, MA (1999).
6. UL 263, *Fire Tests of Building Construction and Materials*, Underwriters Laboratories, Northbrook, IL (1997).
7. T.T. Lie (ed.), *Structural Fire Protection*, American Society of Civil Engineers, New York (1992).
8. *International Fire Engineering Design for Steel Structures: State of the Art*, International Iron and Steel Institute, Brussels, Belgium (1993).
9. *Design of Steel Structures—Part 1-2, General Rules—Structural Fire Design*, CEN, Eurocode 3, Brussels (1995).
10. ASCE/SFPE 29, *Standard Calculation Methods for Structural Fire Protection*, American Society of Civil Engineers (1999).
11. D. Boring, J. Spence, and W. Wells, *Fire Protection through Modern Building Codes*, American Iron and Steel Institute, Washington, DC (1981).
12. D.C. Jeanes, *Technical Report 84-1*, Society of Fire Protection Engineers, Boston (1984).
13. T.Z. Harmathy, NRCC 20956 (DBR Paper No. 1080), National Research Council of Canada, Ottawa (1983).
14. M.S. Abrams, ASTM STP 685, American Society for Testing and Materials, Philadelphia (1979).
15. T.T. Lie, *Fire and Buildings*, Applied Science, London (1972).
16. *Specification for the Design, Fabrication, and Erection of Structural Steel for Buildings*, American Institute of Steel Construction, New York (1978).
17. T.T. Lie and W.W. Stanzak, "Empirical Method for Calculating Fire Resistance of Protected Steel Columns, *Eng. J.*, 57, 5/6, pp. 73-80 (1974).
18. D.R. Boring, *An Analytical Evaluation of the Structural Response of Simply Supported, Thermally Unrestrained Structural Steel Beams Exposed to the Standard Fire Endurance Test*, master's thesis, Ohio State University, Columbus, OH (1970).

19. R.A. Lindberg, *Processes and Materials of Manufacture*, Allyn and Bacon, Boston (1978).
20. D.C. Jeanes, *Methods of Calculating Fire Resistance of Steel Structures*, Engineering Applications of Fire Technology Workshop, SFPE, Boston (1980).
21. H.L. Malhotra, *Design of Fire-Resisting Structures*, Chapman and Hall, New York (1982).
22. T.Z. Harmathy, "A Comprehensive Creep Model," *ASME J. of Basic Eng.*, 89, pp. 496-502 (1967).
23. T.Z. Harmathy, *ASTM STP 422*, American Society for Testing and Materials, Philadelphia (1967).
24. *Fire Resistant Steel Frame Construction*, American Iron and Steel Institute, Washington, DC (1974).
25. *Designing Fire Protection for Steel Columns*, American Iron and Steel Institute, Washington, DC (1980).
26. W.W. Stanzak and T.T. Lie, *Fire Tests on Protected Steel Columns with Different Cross-Sections*, National Research Council of Canada, Ottawa (1973).
27. PABCO, *Pabco Super Firetemp Fireproofing Board Fire Protection Guide*, Ruston, LA (1984).
28. L.G. Seigel, "Designing for Fire Safety with Exposed Steel," *Fire Tech.*, 6, 4, pp. 269-278 (1970).
29. Standard Building Code Congress, *Southern Standard Building Code*, SSB, Birmingham, AL (1985).
30. T.T. Lie and W.W. Stanzak, "Fire Resistance of Protected Steel Columns," *Eng. J. Amer. Inst. Steel Const.*, 10, pp. 82-94 (1973).
31. *Designing Fire Protection for Steel Beams*, American Iron and Steel Institute, Washington, DC (1985).
32. *Load and Resistance Factor Design Specification for Structural Steel Buildings*, American Institute of Steel Construction, New York (1993).
33. *Designing Fire Protection for Steel Trusses*, American Iron and Steel Institute, Washington, DC (1980).
34. *Fire Resistance Design Manual*, Gypsum Association, Evanston, IL (1984).
35. O. Pettersson, S. Magnusson, and J. Thor, *Bulletin 52*, Lund Institute of Technology, Lund, Sweden (1976).
36. G. S. Berger, *Estimating the Temperature Response of Wide Flange Steel Columns in the ASTM E119 Test*, Department of Fire Protection Engineering, University of Maryland, College Park (unpublished) (1987).
37. J.A. Milke, "A Simplified Model for Estimating the Thermal Response of Steel Beam/Concrete Slab Ceiling Assemblies," in *ICFRE2*, SFPE, Bethesda, MD (1997).
38. W.W. Stanzak and T.Z. Harmathy, "Effect of Deck on Failure Temperature of Steel Beams," *Fire Tech.*, 4, 4, pp. 265-270 (1968).
39. I.A. Smith and C. Stirland, "Analytical Methods and Design of Fire Safe Steel Structures," in *International Seminar on Three Decades of Structural Fire Safety*, Borehamwood, UK (1983).
40. *Fire-Safe Structural Steel, A Design Guide*, American Iron and Steel Institute, Washington, DC (1979).
41. M. Law, "Prediction of Fire Resistance," *AISC Eng. J.*, pp. 16-29 (1978).
42. G.V.L. Bond, *Fire and Steel Construction—Water Cooled Hollow Columns*, Constrado (1974).
43. T.T. Lie and T.Z. Harmathy, *Fire Study No. 28*, National Research Council of Canada, Ottawa (1972).
44. W.L. Gamble, "Predicting Protected Steel Member Fire Endurance Using Spreadsheet Programs," *Fire Technology*, 25, 3, pp. 256-273 (1989).
45. O.C. Zienkiewicz, *The Finite Element Method*, McGraw-Hill, New York (1983).
46. M. Paulsson, *TASEF-2*, Lund Institute of Technology, Lund, Sweden (1983).
47. R.H. Iding, Z. Nizamuddin, and B. Bresler, *UCB FRD 77-15*, University of California, Berkeley (1977).
48. A. Anderberg, *PC-TEMPCALC*, Institutet for Brandtekniska, Fragar, Sweden (1985).
49. J.A. Milke, "Estimating Fire Resistance of Tubular Steel Columns," in *Proceedings of Symposium on Hollow Structural Sections in Building Construction*, ASCE, Chicago (1985).
50. K. Bardell, *ASTM STP 826*, American Society for Testing and Materials, Philadelphia (1983).
51. D. Gross, *NBSIR 85-3223*, National Bureau of Standards, Gaithersburg, MD (1985).
52. R. Stubblefield and M.L. Edwards, *NODES-T3: Making FIRES-T3 a Little Easier*, Department of Fire Protection Engineering, University of Maryland, College Park, MD (unpublished) (1991).
53. D.V. Tomecek and J.A. Milke, "A Study of the Effect of Partial Loss of Protection on the Fire Resistance of Steel Columns," *Fire Technology*, 29, 1, pp. 3-21 (1993).
54. A.F. Robertson and J.V. Ryan, "Proposed Criteria for Defining Load Failure of Beams, Floors, and Roof Constructions during Fire Tests," *J. of Res.*, 63C, 2, pp. 121-124 (1959).
55. S. Vinnkota, *Calculation of the Fire Resistance of Structural Steel Members*, ASCE, p. 105 (1979).
56. ECCS, *Fire Resistance of Steel Structures*, ECCS 89, Brussels, Belgium (1995).
57. B.R. Kirby and D.E. Wainman, *The Behaviour of Structural Steelwork in Natural Fires*, British Steel PLC., Rotherham, England (1997).
58. J. Kruppa, "Collapse Temperature of Steel Structures," *J. of Struc. Div.*, 105, pp. 1769-1788 (1979).
59. European Convention for Constructional Steelwork, Technical Committee 3, *European Recommendations for the Fire Safety of Steel Structures*, Elsevier, Amsterdam (1983).
60. A. Chajes, *Principles of Structural Stability Theory*, Prentice-Hall, Englewood Cliffs, NJ (1974).
61. T.T. Lie and W.W. Stanzak, "Structural Steel and Fire: More Realistic Analyses," *AISC Eng. J.*, 13, 2, pp. 35-42 (1976).
62. P.J.E. Sullivan, M.J. Terro, and W.A. Morris, "Critical Review of Fire Dedicated Thermal and Structural Computer Programs," *J. of Applied Fire Science*, 3, 2, pp. 113-135 (1994).
63. D.C. Jeanes, *F. Safety J.*, 9, 1 (1985).
64. J-M. Franssen, J-B. Schleich, L-G Cajot, D. Talamona, B. Zhao, L. Twelt, and K. Both, "A Comparison Between Five Structural Fire Codes Applied to Steel Elements," in *Proceedings of Fourth International Symposium of Fire Safety Science*, International Association of Fire Safety Science, Ottawa, Canada, pp. 1125-1136 (1994).
65. J.M. Franssen, *Étude du Comportement au Feu des Structures Mixtes Ancier—Béton (CEFICOSS)*, A Study of the Behaviour of Composite Steel-Concrete Structures in Fire, Doctoral Dissertation, Université de Liège, Belgium (1987).
66. J.B. Schleich, J.C. Dotreppe, and J.M. Franssen, "Numerical Simulations of Fire Resistance Tests on Steel and Composite Structural Elements on Frames," in *Proceedings of First International Symposium of Fire Safety Science*, Hemisphere Publishing, Gaithersburg, MD, p. 311 (1986).
67. J.A. El-Rimawi, I.W. Burgess, and R.J. Plank, "Model Studies of Composite Building Frame Behaviour in Fire," in *Proceedings of Fourth International Symposium of Fire Safety Science*, International Association of Fire Safety Science, Ottawa, Canada, pp. 1137-1148 (1994).